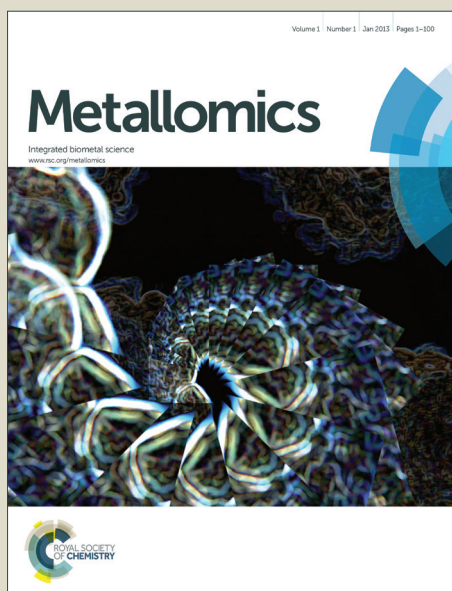


Metallomics

Accepted Manuscript



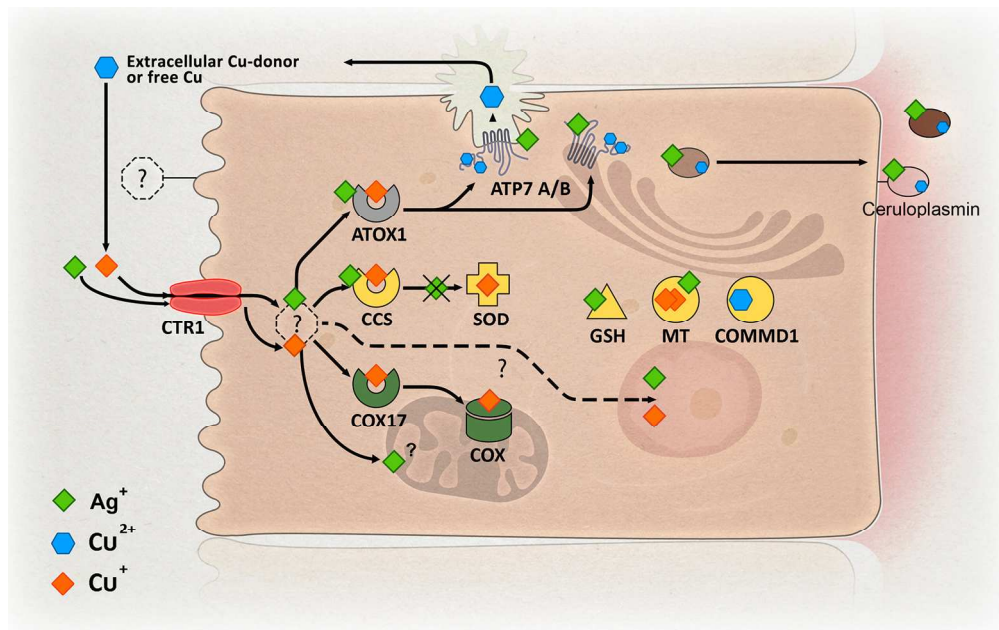
This is an *Accepted Manuscript*, which has been through the Royal Society of Chemistry peer review process and has been accepted for publication.

Accepted Manuscripts are published online shortly after acceptance, before technical editing, formatting and proof reading. Using this free service, authors can make their results available to the community, in citable form, before we publish the edited article. We will replace this *Accepted Manuscript* with the edited and formatted *Advance Article* as soon as it is available.

You can find more information about *Accepted Manuscripts* in the [Information for Authors](#).

Please note that technical editing may introduce minor changes to the text and/or graphics, which may alter content. The journal's standard [Terms & Conditions](#) and the [Ethical guidelines](#) still apply. In no event shall the Royal Society of Chemistry be held responsible for any errors or omissions in this *Accepted Manuscript* or any consequences arising from the use of any information it contains.

1
2
3
4
5
6
7
8
9
10
11
12
13
14
15
16
17
18
19
20
21
22
23
24
25
26
27
28
29
30
31
32
33
34
35
36
37
38
39
40
41
42
43
44
45
46
47
48
49
50
51
52
53
54
55
56
57
58
59
60



160x100mm (300 x 300 DPI)

The effects of silver ions on copper metabolism in rats

²Ilyechova E.Yu., ¹Saveliev A.N., ¹Skvortsov A.N., ³Babich P.S., ¹Zatulovskaia Yu.A., ⁴Pliss M.G., ²Korzhevskii D.E., ²Tsybmalenko N.V., ^{1,2}Puchkova L.V.

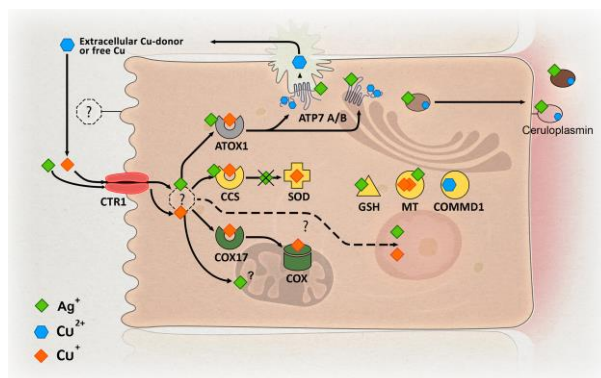
¹Institute of Physics, Nanotechnology, and Telecommunications, St. Petersburg State Polytechnical University, Politekhnicheskaya str., 29, St. Petersburg, 195251 Russia

²Research Institute of Experimental Medicine, Pavlova str., 12, St. Petersburg, 197376 Russia

³Herzen State Pedagogical University of Russia, Kazanskaya (Plekhanova) str., 6, St. Petersburg, 191186 Russia

⁴Scientific Research Institute of Experimental Cardiology and Pharmacology, Morisa Toresa av., 20, box 102, St. Petersburg, 194021 Russia

Table of contents entry



The serum ceruloplasmin-associated copper deficiency induced by silver-containing diet in rats can be compensated by extrahepatic ceruloplasmin synthesis if rats receive silver from birth

Abstract

The influence of short and prolonged diet containing silver ions (Ag-diet) on copper metabolism was studied. Two groups of animals were used: a group of adult rats received Ag-diet for one month (Ag-A1) and another group received Ag-diet for 6 months from birth (Ag-N6). In Ag-A1 rats, the Ag-diet caused dramatic decrease of copper status indexes that was manifested as ceruloplasmin-associated copper deficiency. In Ag-N6 rats, copper status indexes decreased only 2-fold as compared to control rats. In rats of both groups, silver entered bloodstream and accumulated in the liver. Silver was incorporated into ceruloplasmin (Cp), but not SOD1. In the liver, prolonged Ag-diet caused decrease of the expression level of genes, associated with copper

1
2 metabolism. Comparative spectrophotometric analysis of partially purified Cp fractions has
3 shown that Cp from Ag-N6 rats was closer to holo-Cp by specific enzymatic activities and
4 tertiary structure than Cp from Ag-A1 rats. However, Cp of Ag-N6 differs from control holo-Cp
5 and Cp of Ag-A1 by affinity to DEAE-Sepharose and by binding properties to lectins. In
6 bloodstream of Ag-N6, two Cp forms are present as shown in pulse-experiments on rats with
7 liver isolated from circulation. One of Cp isoforms is of hepatic origin, and the other is of extra-
8 hepatic origin; the latter is characterized by faster rate of secretion than hepatic Cp. These data
9 allowed us to suggest that the disturbance of holo-Cp formation in liver was compensated by
10 induction of extra-hepatic Cp synthesis. The possible biological importance of these effects is
11 discussed.

21 Introduction

22
23 Copper is a redox-active and structure cofactor of cuproenzymes catalyzing wide
24 spectrum of biochemical reactions, including oxidative phosphorylation, protection from reactive
25 oxygen species, connective tissue formation, iron bidirectional transport, processing of
26 neuropeptide precursors, and others.¹ Besides, copper takes part in such mechanistic processes as
27 signaling, cellular proliferation, protein secretion through the pathways independent of
28 endoplasmic reticulum and Golgi, neovascularization, carcinogenesis, *i.e.* copper is a secondary
29 messenger.²⁻¹²

30
31 The important physiological roles of copper combine with its high toxicity. The toxicity
32 is caused by the ability of free copper ions to initiate Fenton type reactions and catalyze
33 formation of free radicals. The free radicals generated by these processes then may engage in
34 secondary reactions such as non-selective oxidation of the biomolecules. In physiological
35 conditions, there is no free copper in the cells.¹³ In enzymes, copper is tightly bound by ligand
36 groups of the active centers in both oxidation states. The safe cell traffic of copper to sites of
37 cuproenzyme formation is provided by dedicated cellular metabolic system, which is highly
38 conservative in evolution.¹⁴ Several families of proteins are emerging that help to confine copper
39 to vital roles. They include integral transmembrane transporters and soluble cytoplasmic Cu(I)-
40 chaperone proteins that package copper and guide it to apo-cuproenzymes. The members of this
41 system contain high affinity Cu(I)-binding sites with lower coordination numbers. They can
42 easily pass Cu(I) to each other in the direction of increasing affinity. In this transport system
43 copper is a rapidly delivered cargo, which is not accumulated or exploited. Even minor changes
44 in the structure of the proteins, which take part in copper homeodynamics, result in severe
45 neurodegenerative diseases and cancer.^{15,16} The link between copper metabolism and these
46 disorders is well documented, but the aspects of copper participation in their pathogenesis are not
47
48
49
50
51
52
53
54
55
56
57
58
59
60

1 well understood. The lack of understanding partially results from insufficient knowledge of the
2 precise copper ways from gastrointestinal tract to intracellular sites where copper is inserted into
3 the active centers of enzymes, and the mechanistic processes by which copper drives cellular
4 proliferation and growth. The studies of copper transport in the cell, through the extracellular
5 fluids and between the organs are hampered by methodological problems. They exist partly
6 because radioactive copper isotopes have impractically short half-lives, while the experiments
7 using stable isotope enrichment techniques are often equivocal and hard to interpret.
8

9 About 30 years ago it was shown that intraperitoneal injection of silver nitrate reduced
10 phenoloxidase activity in the extracellular fluids.¹⁷ This finding raised interest to biochemistry of
11 silver and its toxic effects. As a result, it was shown that Ag(I) incorporates into ceruloplasmin
12 (Cp, multicopper blue (ferr)oxidase)¹⁸ and this leads to the loss of its oxidase activity.¹⁹ In the
13 last decades, the identification of Cu(I)-transporter proteins revived the interest to silver
14 bioinorganic chemistry, as abiogenic Ag(I) and essential Cu(I) have the same d^{10} ground state
15 configuration of the valence shell and many similar coordination properties. It was shown that
16 Ag(I) ions coordinate with ligands that are specific to Cu(I) transport both *in vitro* and *in vivo*.²⁰⁻
17
18
19
20
21
22
23
24
25
26
27
28
29
30
31
32
33
34
35
36
37
38
39
40
41
42
43
44
45
46
47
48
49
50
51
52
53
54
55
56
57
58
59
60
23 Thence Ag(I) is used as Cu(I)-like inhibitor in mechanistic studies. Therefore the silver atoms
may be suitable to monitor copper transport pathways. Additionally, the link has been
established between copper level in bloodstream, tumor progression, and platinum
chemotherapy,^{21,24-26} and there is a demand in copper-lowering approaches. So, one of the
possible approaches to manipulate copper status is the use of Ag-treatment.^{21,27-29}

In the present work, the distribution of silver in the organs, liver cells, and blood serum of
rats that received silver with fodder at different stages of development and the effect of Ag-diet
on copper status indexes (Cp activity, Cp protein and copper concentration in serum) were
studied. The properties of Cp isoforms from the serum of these animals were compared. Also the
levels of expression of genes associated with liver copper metabolism were compared. The study
focuses on several groups of genes. The first group consists of cuproenzyme coding genes:
ceruloplasmin (Cp), superoxide dismutase 1 (Sod1, the key component of antioxidant system of
the cell),³⁰ and subunit 4 isoform 1 of cytochrome *c* oxidase (Cox4i1, the subunit is absolutely
required for the assembly of the functional cytochrome *c* oxidase).³¹ The second group includes
the genes encoding copper transporters: high affinity copper transporter CTR1 (Slc31a1, copper
importer through the cell membrane),^{32,33} low affinity copper transporter CTR2 (Slc31a2, copper
transporter from lysosomes to cytosol),³⁴ copper-transporting ATPase (Atp7b, which pumps
copper from cytosol to Golgi complex, where extracellular cuproenzymes are formed),³⁵ and Ccs
(Cu(I)-chaperone that delivers copper to SOD1).³⁶ The third group contains genes, whose
products may participate in copper redox homeodynamics in cytosol. It includes metallothionein

1
2 (Mt1a, which acts both as a donor and acceptor of Cu(I)/Cu(II))³⁷ and Commd1 (Cu(II) binding
3 cytosol protein, which controls the level of intracellular copper by excretion from cells).³⁸ The
4 obtained data may help to understand the details of copper turnover, and may facilitate the
5 development of rational methods for correction of the disorders associated with copper
6 metabolism.
7
8
9

10 **Materials and methods**

11 *Animals and their treatment*

12
13
14
15
16
17
18 Outbred adult 2-month old albino rats purchased from Rappolovo nursery (Leningrad
19 Region, Russia) and the rats born in the vivarium of the Research Institute of Experimental
20 Medicine were used. Groups of 10 or less adult animals, or a female with litter (eight newborns
21 in a litter) were kept in plastic cages (1815 cm² and 720 cm² respectively) with wood cutting
22 waste. The animals were housed with a 12:12-h light-dark cycle in 60% humidity at 22-24 °C,
23 and were given suitable fodder and water *ad libitum*. Procedures involving animals and their care
24 were conducted in conformity with institutional guidelines that are in compliance with national
25 laws (Order N267 of the Ministry of Health of Russian Federation, June 19, 2003; Guide for the
26 Use of Laboratory Animals, Moscow, 2005).
27
28
29
30
31
32

33
34 The experimental rats were fed with fodder containing silver ions (Ag-fodder). To
35 prepare Ag-fodder, AgCl at average dose of 50 mg AgCl per kg of body weight per day was
36 added into ground fodder for rats.²⁸ Supposing that a rat (about 250 g body weight) eats about 30
37 g dry fodder daily, 330 mg of silver ions per 1 kg of fodder were added. Then the fodder was
38 very thoroughly mixed and moistened with distilled water (~ 1:1 w/v). To control uniformity of
39 silver distribution, its concentration was determined in ~100 mg random samples of Ag-fodder
40 dissolved in 1.0 mL HNO₃. The average silver concentration was 1600±160 µg/L (*n* = 4). As
41 indicated by the low standard deviation, silver is quite uniformly distributed in fodder. Therefore
42 the daily intake of silver was regular. In the standard fodder, copper content was 12.5 mg/kg, and
43 so the atomic ratio Ag/Cu was about 15. Two experimental groups were used. The first group
44 (Ag-A1) consisted of five-month old rats that received AgCl with fodder daily during one month.
45 Thus, the action of silver ions began at adult type of copper metabolism (high copper and Cp
46 concentration in blood serum and low copper concentration in the liver). The rats of the second
47 group (Ag-N6) were fed by females, which were receiving Ag-diet from the first day of
48 lactation. The weaned rats were then moved to Ag-diet. In this case the action of silver ions
49 began at embryonic type of copper metabolism (low copper and Cp concentration in serum and
50
51
52
53
54
55
56
57
58
59
60

1
2 high copper level in the liver). Moreover switching of the copper metabolic types occurs amid
3 Ag-diet.³⁹ The rats of the second group were analyzed at the age of 6 months.

4
5 In pulse-experiments, 1.0 mCi of the mixture of [¹⁴C]amino acids (“Isotope”,
6
7
8
9
10
11
12
13
14
15
16
17
18
19
20
21
22
23
24
25
26
27
28
29
30
31
32
33
34
35
36
37
38
39
40
41
42
43
44
45
46
47
48
49
50
51
52
53
54
55
56
57
58
59
60
Czechoslovakia) per 100 g body weight were injected intraperitoneally (*i.p.*). Blood aliquots
were collected from tail vessels through regular time-intervals.

To isolate the liver from circulation, anesthetized rats (1 g of oxybutyrate per 1 kg of
body weight) were subjected to two-step surge. Firstly, a 10 mm incision was made on the neck,
after tissue separation left carotid artery was taken on ligatures; through an incision polyethylene
p 50 catheter was inserted to a depth of 20-25 mm. The distal end of the catheter had a plug
through which radioactive amino acids were injected and blood samples were taken
subsequently. The second step, aimed to isolate the liver from the circulation, was performed as
quickly as possible (about 1 min) using known slightly adapted method.⁴⁰ Briefly, incision (20
mm) was performed in parallel to the upper right costal arch, consistently cutting through the
skin, fascia, and muscles of the abdominal wall to the peritoneum of the rat in the supine position
on heated bedding. Further incision was performed perpendicularly to the dorsal surgical wound
20 mm caudal to the parallel to the spine. The area of inferior *vena cava* and aorta 1-2 mm above
the renal arteries and veins served as a reference for identifying and isolation of hepatic vein and
hepatic artery, then portal vein was found. Common bile duct was identified. Selection was
carried out from the surrounding tissues of the liver so that the body from inside the abdominal
cavity was connected with liver only by stem, containing the common bile duct, portal vein and
the hepatic artery. Applying DeBakey clamp to the hepatic stem performed the complete
isolation of liver from circulation.

Tissue samples and subcellular fractions

The biological samples were collected, snap frozen, and stored at $-70\text{ }^{\circ}\text{C}$ for assessment
of expression of genes, level of proteins, and metals concentration analysis. Blood samples were
collected, clotted, and sera were separated by low-speed sedimentation. To collect urine, the
bladders with urine were carefully removed, put in Eppendorf type tubes, cut into pieces, and
centrifuged at $10,000\times g$ for 5 min. Urine samples were collected as supernatant.

Subcellular fractions were isolated by differential centrifugation. The tissue samples were
homogenized at 0°C in buffer (1:6 w/v respectively) containing 250 mM sucrose, 100 mM KCl,
5 mM MgCl_2 , 10 mM Tris-HCl (pH 7.4), 5 mM DTT, and $0.5\text{ }\mu\text{L/mL}$ of a protease inhibitor
mixture (Sigma, USA) using T10 basic homogenizer 3×20 sec at maximum power (IKA T-10
basic, Germany). Homogenates were centrifuged at $800\times g$ for 10 min. Crude mitochondrial
fraction was separated from postnuclear supernatant as sediment of centrifugation at $12,000\times g$

1
2 for 20 min. Postmitochondrial supernatant was centrifuged at 18,000×g for 60 min. The pellet
3 was a fraction of intracellular membranes; the supernatant comprised cytosol fraction.
4
5

6 7 *Silver-revealing staining of the liver sections*

8
9 Material for histological staining was fixed in the zinc-ethanol-formaldehyde fixative for
10 24 h. After dehydration in ethanol, the material was embedded routinely in paraffin and 5 µm-
11 thick sections were cut. The preparations were stained with hematoxylin, or hematoxylin +
12 eosin.⁴¹ The islets of silver deposit-like matter were imaged by treatment with 5% iodine in
13 ethanol followed by washing with 10% sodium thiosulfate.
14
15
16
17
18

19 20 *Isolation and characteristics of the Cp preparations*

21
22 Serum Cp was isolated by ion-exchange chromatography using DEAE-Sepharose
23 column. The fractions were eluted by step-gradient of NaCl concentration (successively 100,
24 150, 200, 250, and 300 mM NaCl) in 50 mM sodium acetate buffer, pH 5.5.
25
26 Cp samples were characterized by UV-Vis absorption and circular dichroism (CD) spectroscopy.
27
28 The spectra were recorded and processed as described earlier.²⁸
29
30
31

32 33 *Gel-filtration chromatography*

34
35 Cytosol samples (2 mL, total protein content 20 mg/mL) were fractioned by gel-filtration
36 on Sephadex G75 Superfine column (10-40 µm; 1.6×40 cm) in 20 mM Tris-HCl buffer, pH 7.6,
37 containing 5 mM 2-mercaptoethanol. Elution rate was 0.5 mL/min. Blood serum samples (2 mL)
38 were fractionated on the column of the same size with Sephadex G-75 in phosphate saline buffer,
39 pH 7.4. The void volume of the column was estimated using blue dextran. The fractions
40 following the void volume (~1.5 mL per fraction) were collected and specified by A₂₈₀ and A₂₅₄.
41
42
43
44
45

46 47 *Immuno-electrophoresis*

48
49 The following variants of immuno-electrophoresis were used: rocket
50 immuno-electrophoresis, 2D-immuno-electrophoresis, cross-immuno-electrophoresis,⁴² and 2D-
51 affinoimmuno-electrophoresis.⁴³ *Rocket immuno-electrophoresis* was used to measure Cp protein
52 concentration. Briefly, 1% agarose gel containing anti-Cp rabbit polyclonal antibodies (100
53 µg/mL) was prepared in Tris-barbital buffer, pH 8.8 (TBB). Serum aliquots (3 µL) or an
54 appropriate amount of Cp preparation were loaded into wells. Electrophoresis was carried out
55 overnight in TBB at 2 V/cm and 10 – 15 °C. The gels were pressed, dried and stained with *o*-
56 dianisidine and/or Coomassie G-250. The area of the precipitation peak was measured as an area
57 of an isosceles triangle. Rat Cp (A₆₁₀/A₂₈₀=0.045) served as a quantitative standard. 2D-
58
59
60

1
2 *immuno-electrophoresis* was applied to characterize total charge of Cp molecules. For this the
3 samples were fractionated by electrophoresis in 1.2% agarose gel at 10 V/cm on the slides 2.5×7.5
4 cm during 2.5 h (the first direction). The agarose strips were transferred onto the glass plates
5 (6×9 cm); and 1% agarose gel with antibodies to Cp was formed. Then electrophoresis was
6 performed in the second direction at 2 V/cm overnight. *2D-affinoimmuno-electrophoresis* was
7 used to compare the glycan chains of Cp's. The serum samples were pre-incubated with the plant
8 lectins at 4 °C overnight; and then subjected to electrophoresis in the first and second directions
9 as described above. The samples from control and Ag-N6 rats were processed and run in pairs
10 simultaneously at identical conditions. For comparison, the gels were scanned, and the images
11 were superimposed digitally (50%:50% sum), using the sample well as a reference point. *Cross-*
12 *immuno-electrophoresis* was employed to evaluate antigen properties of Cp's. In this case, the
13 samples had to cross agarose strip, containing control rat serum (dissolved 1:100), before
14 entering the agarose gel with antibodies to Cp. Gels were processed as described for rocket
15 immuno-electrophoresis and stained with *o*-dianisidine and then with Coomassie G-250.
16
17
18
19
20
21
22
23
24
25
26
27

28 *Immunoprecipitation*

29
30 Cp was precipitated from 50 µL of rat serum with 500 µL of antibodies to Cp (1 mg/mL).
31 Precipitation was carried out overnight at 4 °C, with constant shaking. Thereafter mixtures were
32 centrifuged at 10,000×g for 20 min; pellets were washed twice with PBS and collected by
33 centrifugation. The pellets were dissolved in 400 µL of pure nitric acid.
34
35
36

37
38 Immunoprecipitation of metallothionein (MT) included two steps. First, 5 µL of
39 antibodies to MT (200 µg/mL) were added to 300 µL of cytosolic fraction and mixtures were
40 incubated overnight at 4 °C with constant mixing. Then 10 µL of rabbit serum and 170 µL of
41 donkey anti-rabbit IgG (secondary antibodies, 1 mg/mL) were added to the mixtures. Rabbit
42 serum was added to enhance precipitation at the second stage. After the overnight incubation,
43 mixtures were treated as described previously.
44
45
46
47
48

49 *Biochemical assays*

50
51 Specific activities of cuproenzymes were detected by the assay-in-gel methods. After non-
52 denaturing PAGE the gels were stained with *o*-dianisidine to reveal the oxidase activity of
53 Cp,⁴⁴ or with Mohr salt/ferrozine system for ferroxidase activity of Cp,⁴⁵ or nitro blue
54 tetrazolium for SOD activity.⁴⁶ Iron-containing ferritin was revealed by staining of gels with 2%
55 K₄Fe(CN)₆ in 2% HCl at room temperature overnight after non-denaturing PAGE. Iron content
56 was estimated by blue staining of electrophoretic bands containing ferritin. The protein loading
57 of the samples was carefully equalized. The respective protein concentrations are indicated in
58
59
60

Figure legends. Gels stained for SOD, Cp ferroxidase and oxidase activities, and iron-loaded ferritin were analyzed by scanning with subsequent digital densitometry (Scion Image software). The results were expressed in arbitrary units. Additionally serum oxidase activity was also determined by Ravin's colorimetric method with *p*-phenylenediamine.⁴⁷ Serum SOD activity was measured by indirect spectrophotometric assay, based on the reaction of superoxide oxidation of quercetin in the presence of TEMED in alkaline medium. Hemoglobin concentration was determined with commercial kit Hemoglobin (ELITechGroup, France) according to the protocol, provided by the manufacturer. Briefly, fresh blood with EDTA was added to Drabkin reagent (0.6 mM potassium ferricyanide, 0.76 mM KCN, 1 mM KH₂PO₄, supplied in the kit) in 1:250 v/v ratios. The cyanmethemoglobin concentration was determined by optical density at 540 nm using calibration curve built for cyanmethemoglobin standards. The standard procedure of semi-quantitative RT-PCR technology was used to evaluate the levels of processed mRNA of the studied genes. Total RNA was isolated using "TRIZOL Reagent" (Invitrogen, UK) in accordance with the manufacturer's procedure. RNA concentration was measured using "NanoDrop 2000" spectrophotometer ("Thermo Scientific", USA). The purity of RNA samples was controlled by optical density ratios A₂₆₀/A₂₈₀. To verify the integrity of the samples, 16S/28S RNA ratio was analyzed after electrophoresis in 1.4% agarose gel with EtBr. The sequences of primers were designed in Primer-BLAST (NCBI, USA): Cp – F: agt aaa caa agt cac aac gag gaa t, R: tcg tat tcc act tat cac caa ttt a (*T_m* 57 °C); Sod1 – F: aca ata cac aag gct gta cca ctg cag g, R: tca tct tgt ttc tcg tgg acc acc ata g (*T_m* 62 °C); Ctr1 – F: tgc cta tga cct tct act ttg g, R: atg aag atg agc atg agg aag t (*T_m* 57 °C); Cox4i1 – F: aag aga gcc att tct act tcg gtg tg, R: cag gct ctc act tct tcc att cat tc (*T_m* 60 °C); Ctr2 – F: gag gct gtg ctt ctc ttt gat t, R: gag cct gta gaa tcc tgg tct g (*T_m* 60 °C); Atp7b – F: cag aag tac ttt cct agc cct agc aag c, R: ccc acc aca gcc aga acc ttc ctg ag (*T_m* 65 °C); Ccs – F: cag tct ggt tgt tga tga ggg aga ag, R: act gaa taa cct gac agg agg ctc tg (*T_m* 60 °C); Mt1a – F: cga ctg cct tct tgt cgc tta cac c, R: tca cat gct cgg tag aaa acg ggg t (*T_m* 58 °C); Commd1 – F: gag ggg aat tct caa gtc tat tgc, R: ctc aga ttc ceg tcc act tct c (*T_m* 60 °C); Fth1 – F: gacagt gct tga acg gaa ccc ggt g, R: tct tca ggg cca cat cat ccc ggt c (*T_m* 62 °C); β-actin – F: gaa gat cct gac cga gcg tg, R: agc act gtg ttg gca tag ag (*T_m* 59 °C). Initial denaturation step lasted for 5 min at 94 °C. PCR reaction lasted for 28 cycles of amplification for β-actin and 30 cycles for all other cDNA (denaturation – 1 min at 94 °C, primer annealing – 1 min, elongation – 1 min at 72 °C). Terminal elongation cycle was held for 7 min. Products after RT-PCR were separated in 1.4% agarose gel with EtBr and analyzed using Scion Image software. The relative levels of mRNAs were calculated using β-actin mRNA as the reference. Each value was combined from 3 independent PCR replicas of cDNA samples, isolated from 3 animals. The results are presented as average values ± standard deviation. Western-blot analysis

1
2 was carried out as described previously.²¹ For calculation of the relative content of
3 immunoreactive polypeptides the membranes with transferred proteins were stained with
4 Ponceau Red, scanned, and the density of 50 kDa bands was used as the concentration
5 reference.⁴⁸ Besides, Ponceau staining served as a control for the quality of the transfer. The
6 analysis was performed for samples from 3 animals.
7
8
9

10
11 In fractions obtained by ion-exchange chromatography, metal atom content per Cp
12 molecule was estimated as follows. Cp concentration in fractions was determined by rocket
13 electrophoresis. Total protein concentration was considered to be not sufficiently accurate
14 estimate of Cp concentration, as the fractions contained some co-eluted proteins. Atomic metal
15 concentration was measured by FAAS (see below) in the whole samples, as it was previously
16 shown that Ag and Cu from serum co-precipitated with Cp.²⁸ Molar metal/protein ratio was then
17 calculated (M_{Cp} was assumed to be 130 kDa).
18
19
20
21
22

23
24 Total radioactivity was determined in serum aliquots at the Whatman 3MM filters as
25 hot TCA-insoluble fraction in mix of 4 g PPO, 0.1 g POPOP in 1 L toluene by liquid
26 scintillation counter (Pharmacia Rackbeta 1209-015, Sweden). Cp-specific radioactivity was
27 determined by immunoprecipitation. For this, 0.5 mg antibodies to Cp were added to 10 μ L
28 serum samples (1.0 mL total volume) and incubated overnight at 4 °C. The precipitates were
29 collected by centrifugation, washed twice with PBS, dissolved in 5% SDS, and put in
30 Whatman 3MM filters to count up radioactivity. Percentage of [¹⁴C]Cp was calculated as %
31 of total radioactivity.
32
33
34
35
36
37

38
39 Specific polyclonal rabbit antibodies were raised against electrophoretically pure rat Cp
40 preparation ($A_{610}/A_{280}= 0.047$) by the method developed by us.⁴⁹ Rabbit antibodies to SOD1 and
41 Cox4i1 were obtained from «Abcam» (UK). Rabbit antibodies to MT and goat antibodies to
42 COMMD1 were purchased from «Santa Cruz Biotechnology» (USA). Antibodies to MT are
43 recommended for detection of all MT isoforms in a broad range of mammalian species including
44 rats. Goat anti-rabbit («Amersham Pharmacia Biotech UK Limited», UK) and donkey anti-goat
45 («Santa Cruz Biotechnology», USA) gamma-globulins, conjugated with horseradish peroxidase
46 were used as secondary antibodies. The immune complexes were visualized by
47 chemiluminescent method, using standard kit Amersham Hyperfilm™ ECL “GE Healthcare”
48 (USA).
49
50
51
52
53
54
55
56
57

58 *Metal concentration measurements*

59
60 Concentrations of copper and silver were measured by FAAS with electrothermal
atomization and Zeeman correction of non-selective absorption on Perkin-Elmer Model 4100ZL
(USA) or ZEE nit 650P (Germany) spectrometers. Tissue samples were weighted and

1
2 homogenized in PBS (1:2 w/v) and dissolved (1:2 v/v) in highly pure concentrated HNO₃
3
4 overnight at 56 °C. Metal concentration in chromatographic fractions and Cp preparations were
5
6 measured without additional processing.

7 Protein concentration was determined by Bradford method.

8
9 Inferences about changes were carried out by Student *t*-test, the changes were considered
10
11 significant at *p* < 0.05. The data are displayed as average value ± standard deviation.
12

13 14 15 **Results**

16 17 18 *1. The effects of the duration of Ag-diet*

19
20 The influence of Ag-diet on selected biochemical indicators was compared in Ag-A1 and
21 Ag-N6 rats. These data are summarized in Table 1. They show that in Ag-A1 rats silver induced
22 dramatic changes in copper status indexes of blood serum. Serum copper concentration was
23 reduced by 90%, while Cp-associated oxidase and ferroxidase activities practically disappeared.
24
25 Meanwhile Cp protein concentration was not affected, as evidenced by rocket
26
27 immunoelectrophoresis. In Ag-N6 rats, the serum copper concentration and the levels of both Cp
28
29 enzymatic activities were reduced 2-fold only. The activities of serum SOD3 and liver cytosolic
30
31 SOD1 were not changed in both Ag-groups. Ag-N6 rats reached fertility at the same age as
32
33 control rats. They could bring viable progeny; however the litter numbers were lower, than in
34
35 control rats (Table 1). To check whether rats of the Ag-N6 group received silver during the early
36
37 postnatal period, the silver distribution in the body of 10-day-old rats fed by Ag-females (Ag-
38
39 P10 rats) was monitored. The data presented in Fig. 1A show that in Ag-P10 rats silver ions enter
40
41 the blood, are accumulated by liver, and excreted with urine. The amount of silver, which was
42
43 present in the bloodstream, corresponded to approximately ½ atom per Cp molecule. Blood
44
45 serum oxidase activity in Ag-P10 rats decreased to ~50% of its level in aged-matched control
46
47 rats (8 ± 0.7 vs 15.3 ± 0.8 mg/dL (*n* = 8), respectively). However, Cp protein concentration
48
49 determined by rocket immunoelectrophoresis did not differ from the control (16.3 ± 1.8 in Ag-
50
51 P10 vs 15.8 ± 1.3 mg/dL (*n* = 8) in the control). Meanwhile, copper accumulation by liver,
52
53 copper concentration in serum and in urine did not change (Fig. 1B). So, in newborns, silver ions
54
55 from milk are capable to metabolic turnover, and they are transferred by the same pathways that
56
57 are characteristic for copper during embryonic type of copper metabolism.³⁹ The data also show
58
59 that Ag-N6 rats received silver before the switching to the adult type of copper metabolism, and
60
noticeable decrease in Cp-associated copper manifested at the 10th day of life.

2. The distribution of silver in the body of Ag-rats

1
2 In Ag-A1 rats, silver was selectively accumulated in the liver (Fig. 2A). In Ag-N6, silver
3 distribution in the body was more even; and its level increased in kidney, spleen, heart, and brain
4 as compared with Ag-A1. In the liver cells of Ag-A1 rats, about 80% silver was localized in the
5 mitochondria (Fig. 2B). In Ag-N6 rats, the silver distribution profile changed: silver was more
6 uniformly distributed between the organelles, but silver concentration was increased many times
7 in cytosol (Fig. 2B).
8

9
10 In Ag-N6, the histological slices of liver, spleen and brain were stained with hematoxylin
11 and eosin or toluidine blue. In spleen and brain, no changes in comparison with control rats were
12 observed (data not shown). However, in the liver of the Ag-N6 animals (Fig. 2D), but not of the
13 Ag-A1 rats (Fig. 2C), yellowish-brown color was observed in the walls of small veins passing
14 the interlobular connective tissue. These vessels were found adjoined with mononuclear cells
15 containing black granules. Treatment of the sections by iodine followed by washing in 10 %
16 sodium thiosulfate resulted in disappearance of the pigmentation, which favors the suggestion of
17 deposition of silver precipitate in intercellular space of wall of the interlobular veins. In the skin
18 of Ag-N6, dark spots could be observed visually after strong illumination of trimmed skin by the
19 lamps for 30 min (Fig. 2F). They are likely to be silver pigmentation. The spots were not
20 observed in Ag-A1 rats (Fig. 2E).
21
22
23
24
25
26
27
28
29
30
31
32

33 34 *3. Distribution of silver in blood serum of Ag-rats and characteristics of partly purified serum* 35 36 *Cp samples*

37
38 Distribution of silver between blood serum proteinaceous components was assessed by
39 gel-filtration. The chromatograms (Fig 3A, B) demonstrate that the largest fraction of serum
40 copper and virtually all serum silver were co-localized in the same peak. This peak corresponds
41 to the protein fraction that contains Cp. The silver to copper ratio was higher in Ag-A1 rats than
42 in Ag-N6 rats. In Ag-A1, there were no lower molecular weight substances that contain silver.
43 The only copper containing peak of the Ag-N6 serum had a distinct shoulder (Fig. 3B), which
44 was not observed in Ag-A1 sera or the sera of intact control rats (our data and⁵¹). The nature of
45 this shoulder was not addressed.
46
47
48
49
50

51
52 Partially purified Cp samples were obtained from the sera of Ag-A1 and Ag-N6 rats by
53 ion-exchange chromatography and their properties were compared (Fig. 3C, D). The
54 chromatographic Cp fractions obtained from the sera of Ag rats were not subject to
55 ethanol:chlorophorm precipitation procedure, as this step caused the loss of copper and silver
56 atoms. So the fractions contained some amount of proteins with relatively low electrophoretic
57 mobilities. Cp bands were prevailing in these samples. The samples displayed different affinity
58 to DEAE-Sepharose. The major fraction of Cp from the serum of Ag-A1 rats was eluted at NaCl
59
60

1
2 concentration 200 and 250 mM. Cp of Ag-N6 rats was eluted at 100 and 150 mM NaCl. In the
3 both Cp preparations, Western blotting after non-denaturing PAGE revealed the presence of two
4 Cp forms, which differed by electrophoretic mobility, but they had the same molecular mass.
5 The major fractions of Cp of the both groups displayed oxidase and ferroxidase activities. Cp
6
7
8
9
10
11
12
13
14
15
16
17
18
19
20
21
22
23
24
25
26
27
28
29
30
31
32
33
34
35
36
37
38
39
40
41
42
43
44
45
46
47
48
49
50
51
52
53
54
55
56
57
58
59
60

concentration 200 and 250 mM. Cp of Ag-N6 rats was eluted at 100 and 150 mM NaCl. In the both Cp preparations, Western blotting after non-denaturing PAGE revealed the presence of two Cp forms, which differed by electrophoretic mobility, but they had the same molecular mass. The major fractions of Cp of the both groups displayed oxidase and ferroxidase activities. Cp samples of Ag-A1 as well as of Ag-N6 contained both copper and silver (Fig. 3E, F). Estimated total amount of metal atoms per Cp molecule comprised approximately 5-6. However, silver content per Cp molecule was ~3 times higher in Ag-A1 group, than in Ag-N6 group.

The fractions with the highest protein concentrations as judged by Western blot analysis (Fig. 3C, fraction 3 and Fig. 3D, fraction 1) were studied by UV-Vis and CD spectroscopy (Fig. 4A, B, respectively). The spectra of analogous holo-Cp preparation are also presented by dotted lines. The UV-Vis spectra were normalized to unity A_{280} . Cp samples from both Ag-groups displayed strongly decreased absorption band at 610 nm and the respective doublet in the CD spectrum, which are characteristic of spectral type I (blue) copper in holo-Cp. A_{610}/A_{280} ratio in Cp sample of Ag-N6 rats comprised 10% of the value for highly pure Cp (0.045), however the shape of 610 nm absorption band was distinctly observed. The negative component of CD doublet was traceable at 450 nm and also comprised ~10% of pure holo-Cp CD. A_{610}/A_{280} ratio in Cp sample from Ag-A1 rats was very low and comprised 1-3% of the value for pure holo-Cp. More precise quantification of A_{610} for this sample was not possible as the band was too faint for accurate resolution of D_{610} into A_{610} and the scattering term. CD in visible region for this sample was also below the used detection limit. Cp samples from both groups of Ag-rats displayed increased absorption at 310-330 nm range, which was absent in the spectrum of holo-Cp or potential impurities, and which was more manifested in Ag-A1 Cp. Near-UV CD spectrum of Cp from Ag-A1 differed strongly from that of holo-Cp and resembled the spectra of partially denatured Cp states⁵² with positive CD at 260 nm and the absence of the negative peak at 280 nm. The spectrum of Cp from Ag-N6 resembled the spectrum of Ag-A1 Cp, but it was slightly shifted towards the spectrum of holo-Cp. However, it could not be modeled by linear combination of Ag-A1 Cp and holo-Cp spectra, so Cp fraction of Ag-N6 rats was not a simple mixture of Ag-A1 Cp with additional amounts of holo-Cp. Far-UV CD spectra generally supported this finding. Secondary structure predictions from far-UV CD spectra were performed by CDNN program; the results refer to the gross protein in the sample. However, as Cp comprised the largest fraction of the sample, the observed large spectral changes corresponded mostly to changes of Cp secondary structure. Cp of Ag-A1 rats differed strongly by secondary structure from holo-Cp (20% α -helix, 30% β -structure, 50% random coil; compare to 12% α , 57% β , 33% random coil in rat holo-Cp CD spectrum). CD spectrum of Cp from Ag-N6 rats and the gross secondary structure (12% α , 47% β , 41% random coil) was roughly in between the

1 values for Ag-A1 Cp and holo-Cp. It means that more Cp molecules in Ag-N6 samples displayed
2 β -structure, characteristic to holo-Cp. As judged by visible spectra, Cp sample of Ag-N6 rats
3 may be regarded as a 1:10-1:8 mixture of blue Cp and non-blue Cp sample of Ag-A1 rats.
4 However, the far-UV CD spectra did not support this idea, as Ag-N6 Cp sample had much less
5 random-coil secondary structures, than the mentioned 1:10 mixture. Therefore, Cp fractions of
6 Ag-N6 and Ag-A1 rats consisted of different conformations of Cp molecules. Cp fractions of
7 Ag-N6 rats evidently contained more blue Cp molecules with intact spectral type I copper, which
8 correspond to higher copper content and (ferr)oxidase activities of blood serum of Ag-N6 rats.
9 But other Cp molecules, which do not absorb at 610 nm, bind silver and/or incomplete number
10 of copper atoms, and most probably lost oxidase activity, are not similar in Ag-N6 and Ag-A1.
11
12
13
14
15
16
17
18
19
20
21

22 4. Some properties of Cp circulating in Ag-N6

23 Cp's total molecular charges, as well as their antigenic and carbohydrate chains identity, were
24 compared in the control and Ag-N6 rats. For this, the variants of immunoelectrophoresis were
25 used (see Methods). The data are presented in Fig. 5. In agarose gel, Cp of both control and Ag-
26 N6 moved as a quite wide single band that formed nearly isosceles triangle when it passed in
27 secondary direction (Fig. 5A). However, the leading shoulder of Cp from Ag-N6 rats lost
28 capability to stain with *o*-dianisidine (Fig. 5B). Cross-immunoelectrophoresis showed that Ag-
29 N6 serum contained Cp isoform with incomplete antigenic identity to holo-Cp (Fig. 5C, D; well
30 2). This Cp isoform lacked oxidase activity, but exhibited affinity to DEAE-Sepharose closest to
31 the control Cp (Fig. 5D, wells 5 and 6). At the same time, oxidase-positive fraction eluted at 100
32 mM NaCl was antigenically closer to holo-Cp of control rats, but showed lower affinity to
33 DEAE-Sepharose (Fig. 5D, well 4).
34
35
36
37
38
39
40
41
42

43 For 2D-affinoimmunoelectrophoresis the following lectins were assayed: (i) concanavalin A
44 (ConA), which has specificity to α -D-mannosyl and α -D-glucosyl groups, (ii)
45 phytohaemagglutinin from kidney red beans, type P (PFP), which has carbohydrate-binding
46 specificity for a complex oligosaccharide containing galactose, *N*-acetylglucosamine, and
47 mannose, and (iii) wheat germ agglutinin (WGA), which binds to *N*-acetyl-D-glucosamine and
48 sialic acid. The data showed that electrophoretic migration of Ag-N6 Cp pre-incubated with
49 ConA was dependent on the quantitative ration between Cp and ConA (Fig. 5E, F). So, Ag-N6
50 Cp migrated faster when 1 μ L of serum aliquots was incubated with 40 μ g ConA (Fig. 5E).
51 However, it moved closer to control Cp, when ConA concentration was 80 μ g per 1 μ L of serum
52 (Fig. 5F). Differential staining with *o*-dianisidine (not shown) and Coomassie produced similar
53 results so only gels stained with Coomassie are shown. These data may possibly indicate that
54 Ag-N6 Cp has less sialic acid residues, since asialo human Cp shows a decrease in affinity for
55
56
57
58
59
60

1
2 ConA.⁵³ Control Cp showed retardation as compared to Ag-N6 Cp after pre-incubation with 120
3 μg of PFP per 1 μL serum (Fig. 5G, H). Besides, staining with *o*-dianisidine and Coomassie G-
4 250 showed heterogeneity of Ag-N6 Cp. Both decrease and increase of PFP concentration did
5 not affect the immunoprecipitation pattern (data not shown). Pre-binding serum with 40 μg of
6 WGA per 1 μL of serum clearly revealed heterogeneity of serum Cp from control rats (Fig. 5I,
7 J). It can be seen that minor fraction of oxidase-negative Cp has low affinity to WGA. It is
8 possible that this Cp form is asialo-Cp. In Ag-N6 serum, oxidase-positive and oxidase-negative
9 Cp forms migrate slower as compared with the corresponding forms of control Cp.
10 The only thing that these data indicate is that the structures of Cp's oligosaccharide moieties of
11 Ag-N6 and control rats differ exactly. Unfortunately information on the fine structures of rat Cp
12 oligosaccharide chains are absent and quantitative theory of glycan/lectin binding is not well
13 developed.
14
15
16
17
18
19
20
21
22
23
24

25 5. The rate of [¹⁴C]Cp secretion in Ag-N6 rats

26
27 Heterogeneous antigenic properties of Cp forms from Ag-N6 as well as their different
28 lectin-binding properties raise question about their origin. So the secretion rate of *de novo*
29 synthesized Cp was traced in the pulse-experiments. In serum, [¹⁴C]proteins appear in 5 min
30 after injection of labeled amino acids (Fig. 6A). At the same time the traces of [¹⁴C]Cp sufficient
31 for its identification by immunoprecipitation appeared in the bloodstream of control rats in 40
32 min, and [¹⁴C]Cp level reached maximum at 90 min (Fig. 6B). The secretion dynamics of Cp
33 coincided well with the data obtained previously.⁵⁴ In Ag-N6 rats, the appearance of [¹⁴C]Cp had
34 two-phase shape (Fig. 6B). The first [¹⁴C]Cp has appeared to the 10th min after the start of
35 experiment, peaking at ~30 min. Another [¹⁴C]Cp form was secreted later. Secretion curve of the
36 latter coincided with the curve for control rats. The results suggest that fast secreted Cp can be of
37 extrahepatic origin. To test this assumption the appearance of radioactive Cp has been traced in
38 rats with liver surgically isolated from circulation. In operated control rats, total serum protein
39 radioactivity was reduced 10-fold (Fig. 6A), it proves that the liver was isolated. In these rats, *de*
40 *nov*o synthesized Cp did not appear in bloodstream for 60 min (Fig. 6C). In Ag-N6 rats subjected
41 to surgery, [¹⁴C]Cp appeared to the 10th min and reached maximum at 30-40 min after pulse-
42 labeling (Fig. 6C). The second stage of secretion was not observed. High proportion of the
43 [¹⁴C]Cp to total radioactivity (4.5%, Fig. 6C) are possibly explained by low total protein
44 radioactivity in operated rats.
45
46
47
48
49
50
51
52
53
54
55
56
57
58
59
60

6. The distribution of silver and copper in liver cytosolic fraction of Ag-N6 rats

1
2 Since prolonged Ag-diet results in silver accumulation in cytosolic fraction (see Fig. 2B) the
3 distribution of silver and copper in cytosolic proteins of control and Ag-N6 rats were studied by
4 gel-filtration. The A_{280} elution profiles were similar in Ag-N6 and control samples. Concretely,
5 the size exclusion chromatogram of control sample is presented in Fig. 7A. It can be seen that the
6 material that absorbs at 280 nm eluted in 4 peaks: 2 major peaks (I and II), minor peak III, and
7 peak IV. Peak III, which contained small proteins, was characterized by increased absorption at
8 254 nm, indicating the presence of cysteine-enriched proteins. The material of peak IV absorbed
9 strongly at 254 nm, this absorption may have been caused by glutathione and/or nucleotides
10 (shoulder of 260 nm peak), as it should in theory contain no proteins, but only low-molecular
11 weight (LMW) components. A_{280} values for the chromatogram of cytosol sample from Ag-N6
12 rats are not presented as they virtually coincided with the profile in Fig 7A.

13 Fractions corresponding to peak maxima (#5 – peak I; #13, #14 – peak II; #18, #20, #22, #25,
14 #27 – peak III, and #37 – peak IV) were analyzed for protein molecular mass by SDS-PAGE
15 (Fig. 7B). The analysis has shown that major peak I contained polypeptides with molecular mass
16 ranging 15-220 kDa. Peak II corresponded to 10-40 kDa polypeptides. Minor peak III covered
17 the range of polypeptides with molecular masses 25-10 kDa (rise, left shoulder), 15-10 kDa
18 (peak) and less than 10 kDa (fall, right shoulder). In peak IV, proteinaceous material was not
19 found. The distribution of molecular weights of polypeptides in the respective chromatographic
20 fractions in Ag-N6 and control cytosols was the same (so only the image for Ag-N6 is shown in
21 Fig. 7B). The fractions were analyzed by non-denaturing PAGE (Fig. 7C, D). Substance, which
22 stained with Coomassie, was found in peak IV of Ag-N6 cytosol, but not in the control (Fig. 7C,
23 D). In parallel, SOD activity was determined by in-gel assays (Fig. 7E, F). In control rats, SOD
24 activity was detected in peaks I and II. The electrophoretic mobility of superoxide scavengers in
25 peak I was lower than in peak II ($R_f \sim 0.14$ and ~ 0.56 , respectively). The activity in peak I may
26 be attributed to extracellular Cu/Zn-SOD (SOD3, homotetramer, 135 kDa).⁵⁵ Cytosolic SOD1
27 (homodimer, 32 kDa) was localized in peak II. MTs were most probably contained in peak III, as
28 they have ~ 10 kDa molecular mass and 30% content of cysteine residues, which corresponded
29 well with increased absorption at 254 nm in peak III. In Ag-N6 rats, some substance also
30 produced a clear band in SOD assay (Fig. 7F) in peak IV. In peak IV, the band stained by
31 Coomassie and the SOD-positive band coincided by electrophoretic mobility ($R_f \sim 0.45$). This
32 band was not observed in control rats (Fig. 7C, E). The treatment of the fraction of peak IV from
33 Ag-N6 rats with SDS and 2-mercaptoethanol at 95 °C resulted in dissociation into LMW
34 substances, which were stained by conventional method with $AgNO_3$ (Fig. 7H, inset), and did
35 not cross-react with antibodies to MT as indicated by Western blotting (data not shown).

1
2
3
4
5
6
7
8
9
10
11
12
13
14
15
16
17
18
19
20
21
22
23
24
25
26
27
28
29
30
31
32
33
34
35
36
37
38
39
40
41
42
43
44
45
46
47
48
49
50
51
52
53
54
55
56
57
58
59
60

Copper distribution between the gel-filtration chromatographic components of cytosol was similar in control and Ag-N6 rats (Fig. 7G, H). Copper was found in major peaks I and II. It is quite possible that copper in peak I belonged to serum proteins (Cp and SOD3), which could contaminate cytosol fraction during homogenization. So, Western blot analysis with antibodies to Cp revealed that peak I contained Cp, additionally, in-gel assay indicated SOD activity in the same peak (Fig. 7B, E, F). Copper in peak II accounted for SOD1 as supported by the SOD in-gel assay (Fig. 7E, F). Copper in minor peak III was most likely bound to MTs, as antibodies to MT precipitated copper from cytosolic fraction of both the control (700 ± 130 $\mu\text{g/L}$; $n=3$) and Ag-N6 (600 ± 80 $\mu\text{g/L}$; $n=3$) rats. Copper content in peak IV was slightly above the background level.

In sample from Ag-N6 rats, silver was detected in peak I (Fig. 7H). This agreed with serum Cp contamination mentioned above, as serum Cp of Ag-rats bears both copper and silver. However, no silver was detected in peak II (Fig. 7H), which corresponded to SOD1 location. Peak III contained silver, which could be firmly attributed to MT fraction, as immunoprecipitates by antibodies to MT contained silver (120 ± 18 $\mu\text{g/L}$; $n=3$). In peak IV, silver content was visibly above the background (Fig. 7H, inset). Thus, in cytosol silver binds to MTs and to yet unidentified substance(s).

7. Expression of genes associated with copper metabolism

We have shown previously that the steady-state levels of mRNAs, encoding proteins associated with copper metabolism, were not affected by silver diet in Ag-A1 rats.²⁷ In Ag-N6, levels of these mRNAs were determined by semi-quantitative RT-PCR; the content of the protein products was determined by immunoblotting (Fig. 8). The relative content of Cp-mRNA did not change in Ag-N6 rats as compared to the control (Fig. 8A). This was in agreement with Western blotting data for Cp (Fig. 8B, C). Ferritin loading with iron did not change either (Fig. 8B, D), according with comparable Cp ferroxidase activity in the two groups (Table 1). It suggested that the Cp-mediated iron transport was retained in Ag-N6 rats. The change in the level of ATP7B-mRNA, the protein product of which takes part in Cp metallation in liver cells, was not significant. The levels of SOD1-mRNA, immunoreactive SOD1 polypeptides, and SOD1-activity did not change in Ag-N6 rats, although the level of mRNA of CCS (Cu-chaperone for SOD1) decreased (Fig. 8). It is known, that there is no correlation between the levels of SOD1-mRNA, apo-SOD1, holo-SOD1 and CCS-mRNA, as CCS-independent pathway of copper delivery to SOD1 exists.⁵⁶ The content of Cox4i1-mRNA, as well as its protein product, decreased concertedly (Fig. 8A–C). The question, if these changes affected mitochondrial function, was beyond the scope of this work. The levels of MT1a-mRNA and COMMD1-mRNA decreased in Ag-N6 rats as compared to the control; meanwhile the content of the respective

1
2 products did not change (Fig. 8A–C). For MT this inconsistency may arise, because primers
3 were used for MT1a isoform, while antibodies detected a range of MT isoforms. For COMMD1,
4 retarded ubiquitin-mediated COMMD1 degradation could be induced by changes in copper
5 turnover.³ The mRNA levels for two major Cu(I)/Ag(I)-transporters CTR1/2, which control
6 copper import and recycling were decreased in Ag-N6. So, prolonged Ag-diet causes the
7 decrease of the activity of the genes, the products of which participate in copper homeodynamics
8 (CTR1, CTR2, CCS, MT, COMMD1) in the liver. Additional investigations are required to
9 understand complex relationships between Cu/Ag concentrations and expression levels of these
10 genes.
11
12
13
14
15
16
17
18
19

20 Discussion

21 Since silver ions are promising for use in the research of copper homeodynamics in the
22 whole body and in the cells of various organs, as well as a possible agent that causes highly
23 specific deficit of extracellular copper,²¹ we investigated the effects of silver ions on copper
24 metabolism depending on the duration of silver action. *In vitro* and *in vivo* investigations usually
25 base on the application of well-soluble silver nitrate. But this does not take into account that
26 immediately after injection AgNO₃ is converted to AgCl and toxic nitrates. In this work, AgCl
27 was added to standard fodder. This approach has several advantages. First, despite well-known
28 low solubility of AgCl in water, silver ion is easily mobilized from AgCl in the gastrointestinal
29 tract, where many small nucleophilic molecules are present, which coordinate Ag(I) better than
30 Cl⁻ or H₂O and make it soluble. Second, the large dose of AgNO₃ forms large quantities of toxic
31 HNO₃. On the contrary, AgCl-containing diet guarantees mild continuous physiological Ag(I)
32 assimilation by CTR1. The use of AgCl allowed us to carry out chronic experiment, when rats
33 received silver from birth for 6 months and did not display any signs of toxicosis (about 30
34 animals in total were under observation). This long experiment allowed us to compare the effect
35 of silver ions on copper metabolism during different stages of development without blocking it
36 completely or inducing acute copper deficiency.
37
38
39
40
41
42
43
44
45
46
47
48
49

50 In the adult rats, complete serum Cp-associated copper deficiency developed after 1
51 month of Ag-diet. Cp-specific activities in blood serum were below detection levels,
52 conformation of Cp molecules was altered, and the Ag-A1 rats lost the ability to bring viable
53 progeny. However, the activities of SOD1, SOD3 (Table 1) and COX²¹ were not changed. No
54 other detrimental health effects were observed besides the loss of fertility.⁵⁰
55
56
57
58

59 In the Ag-N6 rats, complete holo-Cp deficiency did not occur, Cp oxidase and
60 ferroxidase activities were reduced only 2-fold. Ag-N6 rats could bring viable progeny, although
the litter numbers were reduced ~2 fold. Basing on these observations we can conclude the

1 following. First, serum Cp is the essential copper source for the developing rat embryos. This
2 conclusion corresponds to the data, obtained on mice with Cp^{-/-} genotype. Cp-deficient mice
3 brought half those of pups from wild type dams, and normal copper accumulation in the liver of
4 fetuses and newborns was disturbed.⁵⁷ Second, accumulation of copper in the liver during
5 embryonic and early postnatal development is a very important process, which possibly can
6 adjust the copper balance in copper-deficient ecological conditions. This adjustment may include
7 the induction of alternative copper transport pathways, due to which Cp-associated copper
8 deficiency is compensated.

9
10
11
12
13
14
15
16
17
18
19
20
21
22
23
24
25
26
27
28
29
30
31
32
33
34
35
36
37
38
39
40
41
42
43
44
45
46
47
48
49
50
51
52
53
54
55
56
57
58
59
60

The evidence for the presence of such pathways is rather high oxidase-positive Cp level in the Ag-N6 rats, which comprises 50% of physiological value despite the high persisting levels of silver (Table 1). The expression levels of Cp gene in liver were virtually the same in Ag-A1, Ag-N6, and in the control group (Fig. 8). At the same time serum Cp of Ag-A1 and Ag-N6 differ by some indicators. First, they display different content of silver atoms per Cp molecule (Fig. 3E, F). On the contrary, gross secondary structure of Cp from the Ag-N6 rats was much closer to that of holo-Cp, and some of the blue active sites were correctly loaded with copper (Fig. 4). Second, serum Cp from Ag-A1 and Ag-N6 demonstrated different affinities to DEAE-Sepharose (Fig. 3). This property is primarily determined by the number and complexity of oligosaccharide chains. The data about the fine structure of oligosaccharide chains are available only for human Cp, and it was shown that rat Cp glycan chains are alike, but not identical to them.⁵⁸ Normal human holo-Cp produced by liver contains biantennary and triantennary oligosaccharide chains with 5 NANA residues. Maturation of Cp oligosaccharide chains, like that of all N-glycoproteins, occurs in trans-Golgi compartment, where insertion of copper into Cp active sites also occurs.⁵⁹ Cp from Ag-A1 rats was practically identical to holo-Cp by affinity to DEAE-Sepharose, which evidences the presence of mature oligosaccharide chains. Basing on UV-Vis absorption and CD spectra, Cp molecules from Ag-A1 rats had abnormal secondary structure and no copper in blue catalytic sites. Hence, maturation of oligosaccharide chains does not depend on the active centers formation. Third, lectin-binding properties of Cp glycan chains of Ag-N6 and control rats are not similar (Fig. 5E–J). Fourth, serum protein of Ag-N6 rats contains a Cp isoform that is not completely identical by its antigenic properties to Cp of control rats (Fig. 5C, D). Fifth, Ag-N6 serum contains Cp of extrahepatic origin (Fig. 6). With great caution we can think that, in Ag-N6, oxidase-positive Cp with the lowest affinity to DEAE-Sepharose (100 mM NaCl fraction) is extrahepatic Cp, while oxidase-negative Cp fraction, which exhibits a greater affinity for DEAE-Sepharose, is the liver Cp. The fact that silver/copper initially enters the liver and is incorporated into Cp allows us to think so. Unfortunately, it is impossible to assume exactly what Cp isoform has extrahepatic origin, or whether this Cp form has altered glycan chains. It is neither possible

1
2 to tell what Cp isoform demonstrated oxidase activity because the rapidly secreted Cp isoform
3 was registered by radioactivity and it could not be segregated in the analysis. Despite these
4 difficulties we can confidently assume that the deficiency of Cp-associated copper at early stages
5 of ontogenesis may induce non-hepatic Cp synthesis. Possibly, the leukocytes compensate the
6 deficiency of oxidase-positive Cp level. This assumption can be made, because leukocytes and
7 macrophages contain mature transcripts of Cp-mRNA.^{60,61} The observed ~30 min delay between
8 the injection of [¹⁴C]amino acids and the peak of labeled Cp in bloodstream of Ag-N6 was
9 theoretically enough for synthesis, maturation, and secretion of holo-Cp molecules. Translation
10 rate is 3-5 codons/s, and full-length Cp polypeptide has ~1060 amino acid residues, so the
11 complete Cp polypeptide can be synthesized in 4 – 6 min; some time is also needed for its
12 metallation and glycosylation. For comparison, radioactively pulse-labeled albumin peak appears
13 in bloodstream at 8 – 10 min after [¹⁴C]amino acids injection.⁶² Radioactive hepatic Cp appeared
14 in bloodstream to 60-90 min (Fig. 6B), while ‘extrahepatic’ Cp peaked at 30 – 40 min. It is likely
15 that ‘extrahepatic’ Cp is secreted constitutively, contrary to the liver, where mature Cp is
16 accumulated in secretory vesicles of trans-Golgi network.²⁸

17
18 We suppose that, in adult rats, Ag-diet causes selective accumulation of silver in the liver,
19 inclusion of silver ions into Cp, and formation of Cp-associated copper deficiency. In rats that
20 started to receive silver from birth, at postnatal stage with embryonic type copper metabolism,
21 extrahepatic Cp synthesis and secretion are induced. Therefore Ag-N6 rats retain fertility (Table
22 1). For comparison, feeding of female rats with Ag-diet throughout the term resulted in the
23 developmental abnormalities of embryos; prenatal death or the 100% mortality of the newborns
24 in the first 24 h of life was observed.⁵⁰ Possibly, an alternative pattern of Cu/Ag routes produces
25 more uniform silver distribution in the organs of Ag-N6 rats, and results in silver inclusions in
26 extracellular space (Fig. 2). The existence of alternative copper transport pathways, which are
27 activated by copper deficient state, is supported by other findings, e.g. *in vivo* and *in vitro*
28 models with *CTR1* gene knockout.⁶³⁻⁶⁵ In order to track these pathways, additional experiments
29 are required.

30
31 Inside the liver cells, in rats of both experimental groups, silver was accumulated in
32 mitochondria (Fig. 2). This fact agrees with the developing concept that mitochondria play key
33 role in the homeodynamics of copper. It is known that under elevated cytosolic copper
34 concentrations (e.g., patients with Wilson disease or LEC rats, and *ATP7B*^{-/-} mice), Cu(I) is
35 chelated by LMW substance and transported to mitochondrial matrix through the mitochondrial
36 carrier family protein.^{66,67} Besides mitochondria, silver ions were found in MT. These data are in
37 good agreement with the ability of MT to bind silver.⁶⁸ In Ag-N6 cytosol, we found unidentified
38 LMW substance that accumulated silver ions (Fig. 7). These data suggest that Ag-animals may
39
40
41
42
43
44
45
46
47
48
49
50
51
52
53
54
55
56
57
58
59
60

1
2 be a valuable model for studying intracellular Cu(I) routes and the role of mitochondria in
3
4 controlling cytosolic Cu(I) concentration.

5
6 We have distinctly shown that silver was included into Cp and blocked the formation of
7
8 its functional active sites. Meanwhile silver was not included into SOD1 (most probably it was
9
10 neither included into SOD3), and did not change either activities (Table 1 and Fig. 7). This fact
11
12 can be explained well taking into account the difference between active sites of these
13
14 cuproenzymes, and the theory of hard and soft acids and bases (Pearson's HSAB principle). In
15
16 both SODs copper in the active sites is coordinated by histidine residues only, which are electron
17
18 donors with intermediate hardness, and good ligands for Cu(II). However, they are not so good
19
20 at stabilizing Ag(I), which is a soft acceptor. The trinuclear center of Cp, which is an oxygen-
21
22 reducing site, also contains only histidine residues (Table 2). However, Cp molecule also has 3
23
24 blue copper sites, each blue site contains a key cysteine residue. Cysteine is a soft donor and is
25
26 good at stabilizing both Cu(I) and Ag(I); this property is widely exploited in Cu(I)-chaperones.
27
28 The process of transfer of Cu(I) from chaperone to histidine sites is somehow coupled with
29
30 copper oxidation to Cu(II). This process is not possible for Ag(I), so silver cannot be inserted
31
32 into Cu/Zn-SODs, and no inactivated SOD molecules are observed. Cysteine-containing sites of
33
34 Cp may adopt silver, however, it cannot oxidize; this fact alone should render Cp inactive.

35
36 As a summary we may conclude that the studied rat models with controlled Cp-associated
37
38 copper deficiency provoked by silver ions is perspective (1) for mechanistic studies of copper
39
40 transport, (2) for understanding of mechanisms of copper distribution in the mammalian
41
42 organism and (3) in the cell, as well as (4) for analysis of cuproenzyme active center formation.

43 44 **Acknowledgements**

45
46 The work was supported by RFBR grants 09-04-01165-a (PLV), 12-04-01530-a (PLV), 12-04-
47
48 31518 (IEYu), 14-04-01640 (NVT). The authors thank Michael Rusakov for help in the design
49
50 of the graphical abstract.
51
52
53
54
55
56
57
58
59
60

References

1. H. Tapiero, D.M. Townsend and K.D. Tew, Trace elements in human physiology and pathology. Copper, *Biomed. Pharmacother.*, 2003, **57**, 386–398.
2. I. Prudovsky, F. Tarantini, M. Landriscina, D. Neivandt, R. Sold, A. Kirov, D. Small, K.M. Kathir, D. Rajalingam and T.K.S. Kumar, Secretion Without Golgi, *J. Cell. Biochem.*, 2008, **103**, 1327–1343.
3. A.R. Mufti, E. Burstein and C.S. Duckett, XIAP: cell death regulation meets copper homeostasis, *Arch. Biochem. Biophys.*, 2007, **463**, 168–174.
4. C. Cursiefen, L. Chen, L.P. Borges, D. Jackson, J. Cao, C. Radziejewski, P.A. D'Amore, M.R. Dana, S.J. Wiegand and J.W. Streilein, VEGF-A stimulates lymphangiogenesis and hemangiogenesis in inflammatory neovascularization via macrophage recruitment, *J. Clin. Invest.*, 2004, **113**, 1040–1050.
5. F. Fan, J.S. Wey, M.F. McCarty, A. Belcheva, W. Liu, T.W. Bauer, R.J. Somcio, Y. Wu, A. Hooper, D.J. Hicklin and L.M. Ellis, Expression and function of vascular endothelial growth factor receptor-1 on human colorectal cancer cells, *Oncogene*, 2005, **24**, 2647–2653.
6. A.D. Yang, E.R. Camp, F. Fan, L. Shen, M.J. Gray, W. Liu, R. Somcio, T.W. Bauer, Y. Wu, D.J. Hicklin and L.M. Ellis, Vascular endothelial growth factor receptor-1 activation mediates epithelial to mesenchymal transition in human pancreatic carcinoma cells, *Cancer Res.*, 2006, **66**, 46–51.
7. F. Martin, T. Linden, D.M. Katschinski, F. Oehme, I. Flamme and C.K. Mukhopadhyay, Copper-dependent activation of hypoxia-inducible factor (HIF)-1: implications for ceruloplasmin regulation, *Blood*, 2005, **105**, 4613–4619.
8. C. Gérard, L.J. Bordeleau, J. Barralet and C.J. Doillon, The stimulation of angiogenesis and collagen deposition by copper, *Biomaterials*, 2010, **31**, 824–31.
9. S.L. Payne, M.J. Hendrix and D.A. Kirschmann, Paradoxical roles for lysyl oxidases in cancer – a prospect, *J. Cell Biochem.*, 2007, **101**, 1338–1354.
10. R. Ioannoni, J. Beaudoin, L. Lopez-Maury, S. Codlin, J. Bahler and S. Labbe, Cuf2 is a novel meiosis-specific regulatory factor of meiosis maturation, *PLoS One*, 2012, **7**, e36338. doi: 10.1371/journal.pone.0036338.
11. V. Gogvadze, B. Zhivotovsky and S. Orrenius, The Warburg effect and mitochondrial stability in cancer cells, *Mol. Aspects Med.*, 2010, **31**, 60–74.
12. M.L. Turski, D.C. Brady, H.J. Kim, B.E. Kim, Y. Nose, C.M. Counter, D.R. Winge and D.J. Thiele, A novel role for copper in Ras/mitogen-activated protein kinase signaling, *Mol. Cell Biol.*, 2012, **32**, 1284–1295.
13. T.D. Rae, P.J. Schmidt, R.A. Pufahl, V.C. Culotta and T.V. O'Halloran, Undetectable intracellular free copper: the requirement of a copper chaperone for superoxide dismutase, *Science*, 1999, **284**, 805–808.
14. M.R. Bleackley and R.T. Macgillivray, Transition metal homeostasis: from yeast to human disease, *Biomaterials*, 2011, **24**, 785–809.

- 1
2
3
4
5
6
7
8
9
10
11
12
13
14
15
16
17
18
19
20
21
22
23
24
25
26
27
28
29
30
31
32
33
34
35
36
37
38
39
40
41
42
43
44
45
46
47
48
49
50
51
52
53
54
55
56
57
58
59
60
15. E. Gaggelli, H. Kozlowski, D. Valensin and G. Valensin, Copper homeostasis and neurodegenerative disorders (Alzheimer's, prion, and Parkinson's diseases and amyotrophic lateral sclerosis), *Chem. Rev.*, 2006, **106**, 1995–2044.
16. A. Southon, R. Burke and J. Camakaris, What can flies tell us about copper homeostasis? *Metalloomics*, 2013, **5**, 1346–1356.
17. T. Pribyl, J. Jahodová and V. Schreiber, Partial inhibition of oestrogen-induced adenohypophyseal growth by silver nitrate, *Horm. Res.*, 1980, **12**, 296–303.
18. J.R. Prohaska, Impact of copper limitation on expression and function of multicopper oxidases (ferroxidases), *Adv. Nutr.*, 2011, **2**, 89–95.
19. F. Hirasawa, Y. Kawarada, M. Sato, S. Suzuki, K. Terada, N. Miura, M. Fujii, K. Kato, Y. Takizawa and T. Sugiyama, The effect of silver administration on the biosynthesis and the molecular properties of rat ceruloplasmin, *Biochim. Biophys. Acta*, 1997, **1336**, 195–201.
20. J. Bertinato, L. Cheung, R. Hoque and L.J. Plouffe, Ctr1 transports silver into mammalian cells, *J. Trace Elem. Med. Biol.*, 2010, **24**, 178–184.
21. E.A. Zatulovskiy, A.N. Skvortsov, P. Rusconi, E.Y. Ilyechova, P.S. Babich, N.V. Tsymbalenko, M. Brogginini and L.V. Puchkova, Serum depletion of holo-ceruloplasmin induced by silver ions in vivo reduces uptake of cisplatin, *J. Inorg. Biochem.*, 2012, **116**, 88–96.
22. M.J. Petris, K. Smith, J. Lee and D.J. Thiele, Copper-stimulated endocytosis and degradation of the human copper transporter, hCtr1, *J. Biol. Chem.*, 2003, **278**, 9639–9646.
23. U.N. Kommuguri, S. Bodiga, S. Sankuru and V.L. Bodiga, Copper deprivation modulates CTR1 and CUP1 expression and enhances cisplatin cytotoxicity in *Saccharomyces cerevisiae*, *J. Trace Elem. Med. Biol.*, 2012, **26**, 13–19.
24. S. Ishida, J. Lee, D.J. Thiele and I. Herskowitz, Uptake of the anticancer drug cisplatin mediated by the copper transporter Ctr1 in yeast and mammals, *Proc. Natl. Acad. Sci. U.S.A.*, 2002, **99**, 14298–14302.
25. S. Ishida, F. McCormick, K. Smith-McCune and D. Hanahan, Enhancing tumor-specific uptake of the anticancer drug cisplatin with a copper chelator, *Cancer Cell*, 2010, **17**, 574–583.
26. S.S. More, O. Akil, A.G. Ianculescu, E.G. Geier, L.R. Lustig and K.M. Giacomini, Role of the copper transporter, CTR1, in platinum-induced ototoxicity, *J. Neurosci.*, 2010, **30**, 9500–9509.
27. S.A. Klotchenko, N.V. Tsymbalenko, K.V. Solov'ev, A.N. Skvortsov, E.A. Zatulovskii, P.S. Babich, N.A. Platonova, M.M. Shavlovskii, L.V. Puchkova and M. Brogginini, The effect of silver ions on copper metabolism and expression of genes encoding copper transport proteins in rat liver, *Dokl. Biochem. Biophys.*, 2008, **418**, 24–27.
28. E. Ilyechova, A. Skvortsov, E. Zatulovsky, N. Tsymbalenko, M. Shavlovsky, M. Brogginini and L. Puchkova, Experimental switching of copper status in laboratory rodents, *J. Trace Elem. Med. Biol.*, 2011, **25**, 27–35.
29. P.S. Babich, A.N. Skvortsov, P. Rusconi, N.V. Tsymbalenko, M. Mutanen, L.V. Puchkova and M. Brogginini, Non-hepatic tumors change the activity of genes encoding copper trafficking proteins in the liver, *Cancer Biol. Ther.*, 2013, **14**, 614–624.

- 1
2
3
4
5
6
7
8
9
10
11
12
13
14
15
16
17
18
19
20
21
22
23
24
25
26
27
28
29
30
31
32
33
34
35
36
37
38
39
40
41
42
43
44
45
46
47
48
49
50
51
52
53
54
55
56
57
58
59
60
30. I.N. Zelko, T.J. Mariani and R.J. Folz, Superoxide dismutase multigene family: A comparison of the CuZn-SOD (SOD1), Mn-SOD (SOD2), and EC-SOD (SOD3) gene structures, evolution, and expression, *Free Radical Biology and Medicine*, 2002, **33**, 337–349.
31. O.-M. H. Richter and B. Ludwig, Cytochrome *c* oxidase – structure, function, and physiology of redox-driven molecular machine, *Rev. Physiol. Biochem. Pharmacol*, 2003, **147**, 47–74.
32. Y. Wang, V. Hodgkinson, S. Zhu, G.A. Weisman and M.J. Petris, Advances in the understanding of mammalian copper transporters, *Adv. Nutr.*, 2011, **2**, 129–137.
33. A.N. Skvortsov, E.A. Zatulovskiy and L.V. Puchkova, Structure-functional organization of eukaryotic high-affinity copper importer CTR1 determines its ability to transport copper, silver, and cisplatin, *Mol. Biol. (Moscow, Russ. Fed., Engl. Ed.)*, 2012, **46**, 304–315.
34. P.V.E. van den Berghe, D.E. Folmer, H.E.M. Malingre, E. van Beurden, A.E.M. Klomp, B. van de Sluis, M. Merckx, R. Berger and L.W.J. Klomp, Human copper transporter 2 is localized in late endosomes and lysosomes and facilitates cellular copper uptake, *Biochem. J.*, 2007, **407**, 49–59.
35. S. Lutsenko, A. Gupta, J.L. Burkhead and V. Zuzel, Cellular multitasking: The dual role of human Cu-ATPases in cofactor delivery and intracellular copper balance, *Arch. Biochem. Biophys.*, 2008, **476**, 22–32.
36. A.L. Caruano-Yzermans, T.B. Bartnikas and J.D. Gitlin, Mechanisms of the copper-dependent turnover of the copper chaperone for superoxide dismutase, *J. Biol. Chem.*, 2006, **281**, 13581–13587.
37. A.E. Nielsen, A. Bohr and M. Penkowa, The balance between life and death of cells: roles of metallothioneins, *Biomark. Insights*, 2007, **1**, 99–111.
38. H. Fieten, P.A.J. Leegwater, A.L. Watson and J. Rothuizen, Canine models of copper toxicosis for understanding mammalian copper metabolism, *Mamm. Genome*, 2012, **23**, 62–75.
39. L.S. Hurley, C.L. Keen and B.O. Lonnerdal, Copper in fetal and neonatal development, *Hunt Ciba Foundation Symp.*, 1980, 227–245.
40. J. Belghiti, S. Dokmak and K. Paugam-Burtz, Vascular isolation techniques in liver resection, in *Recent Advances in Liver Surgery*, ed. by Dionigi R., Landes Bioscience, 2009, pp. 80–97.
41. D.E. Korzhevskii, E.G. Sukhorukova, E.G. Gilerovich, E.S. Petrova, O.V. Kirik and I.P. Grigor'ev, Advantages and disadvantages of zink-ethanol-formaldehyde as a fixative for immunocytochemistry and confocal laser microscopy, *Morfologiia*, 2013, **143**, 81–85.
42. I. Kroll, in *A manual of quantitative immuno-electrophoresis*. Ed. by N.H. Axelsen, J.Kroll, B.Weeke, Oslo-Bergen-Troms, Universitet Storlaget, 1973.
43. J.-E.S. Hansen, P.M.H. Heegaard, S.P. Jensen, B. Nargaard-Pedersen and T.C. Bag-Hansen, Heterogeneity in copper and glycan content of ceruloplasmin in human serum differs in health and disease, *Electrophoresis*, 1988, **9**, 273–278.
44. J.A. Owen and H. Smith, Detection of ceruloplasmin after zone electrophoresis, *Clin. Chim. Acta*, 1961, **6**, 441–444.

- 1
2 45. H. Chen, Z.K. Attieh, T. Su, B.A. Syed, H. Gao, R.M. Alaeddine, T.C. Fox, J. Usta, C.E.
3 Naylor, R.W. Evans, A.T. McKie, G.J. Anderson and C.D. Vulpe, Hephæstín is a ferroxidase
4 that maintains partial activity in sex-linked anemia mice, *Blood*, 2004, **103**, 3933–3939.
5
6 46. C. Vives-Bauza, A. Starkov and E. Garcia-Arumi, Measurements of the antioxidant enzyme
7 activities of superoxide dismutase, catalase, and glutathione peroxidase, *Methods Cell Biol.*,
8 2007, **80**, 379–393.
9
10 47. H.A. Ravin, An improved colorimetric enzymatic assay of ceruloplasmin, *J. Lab. Clin. Med.*,
11 1961, **58**, 161–168.
12
13 48. G.M. Aldridge, D.M. Podrebarac, W.T. Greenough and I.J. Weiler, The use of total protein
14 stains as loading controls: an alternative to high-abundance single-protein controls in semi-
15 quantitative immunoblotting, *J. Neurosci. Methods*, 2008, **172**, 250–254.
16
17 49. V.S. Gaitskhoki, V.M. L'vov, N.K. Monakhov, L.V. Puchkova, A.L. Schwartzman, L.Ju.
18 Frolova, N.A. Skobeleva, W. Zagorski and S.A. Neifakh, Intracellular distribution of rat-liver
19 polyribosomes synthesizing ceruloplasmin, *Eur. J. Biochem.*, 1981, **115**, 39–44.
20
21 50. M.M. Shavlovski, N.A. Chebotar, L.A. Konopistseva, E.T. Zakharova, A.M. Kachourin,
22 V.B. Vassiliev and V.S. Gaitskhoki, Embryotoxicity of silver ions is diminished by
23 ceruloplasmin – further evidence for its role in the transport of copper, *Biometals*, 1995, **8**, 122–
24 128.
25
26 51. A. Cabrera, E. Alonzo, E. Sauble, Y.L. Chu, M.C. Linder, D.S. Sato and A.Z. Mason,
27 Copper binding components of blood plasma and organs, and their responses to influx of large
28 doses of ⁶⁵Cu, in the mouse, *Biometals*, 2008, **21**, 525–543.
29
30 52. M. Noyer and F. W. Putnam, A circular dichroism study of undegraded human
31 ceruloplasmin, *Biochemistry*, 1981, **20**, 3536–3542.
32
33 53. E. L. Saenko, V.V. Basevich and A.I. Yaropolov, Interaction of human ceruloplasmin with
34 immobilized plant lectins, *Biopolymers and Cell [Rus]*, 1989, **5**, 52–57.
35
36 54. N.E. Hellman, S. Kono, H. Miyajima and G.D. Gitlin, Biochemical analysis of missense
37 mutation in aceruloplasminemia, *J. Biol. Chem.*, 2002, **277**, 1375–1380.
38
39 55. S.L. Marklund, Human copper-containing superoxide dismutase of high molecular weight,
40 *Proc. Natl. Acad. Sci. USA*, 1982, **79**, 7634–7638.
41
42 56. K.W. Sea, Y. Sheng, H.L. Lelie, L. Kane Barnese, A. Durazo, J.S. Valentine and E.B. Gralla,
43 Yeast copper-zinc superoxide dismutase can be activated in the absence of its copper chaperone,
44 *J. Biol. Inorg. Chem.*, 2013, **18**, 985–992.
45
46 57. Y.L. Chu, E.N. Sauble, A. Cabrera, A. Roth, M.L. Ackland, J.F. Mercer and M.C. Linder,
47 Lack of ceruloplasmin expression alters aspects of copper transport to the fetus and newborn, as
48 determined in mice, *Biometals*, 2012, **25**, 373–382.
49
50 58. E.T. Zakharova, V.B. Vasil'ev, V.N. Gorbunova and M.M. Shavlovskii, Isolation and
51 physico-chemical properties of rat ceruloplasmin, *Biokhimiia*, 1983, **48**, 1709–1720.
52
53 59. G. Loudianos and J.D. Gitlin, Wilson's disease, *Semin. Liver Dis.*, 2000, **20**, 353–364.
54
55
56
57
58
59
60

- 1
2
3
4
5
6
7
8
9
10
11
12
13
14
15
16
17
18
19
20
21
22
23
24
25
26
27
28
29
30
31
32
33
34
35
36
37
38
39
40
41
42
43
44
45
46
47
48
49
50
51
52
53
54
55
56
57
58
59
60
60. J. Banha, L. Marques, R. Oliveira, M. Martins, E. Paixão, D. Pereira, R. Malhó, D. Penque and L. Costa, Ceruloplasmin expression by human peripheral blood lymphocytes: A new link between immunity and iron metabolism, *Free Radical Biol. Med.*, 2008, **44**, 483–492.
61. B. Bakhautdin, M. Febbraio, E. Goksoy, C.A. de la Motte, M.F. Gulen, E.P. Childers, S.L. Hazen, X. Li and P.L. Fox, Protective role of macrophage-derived ceruloplasmin in inflammatory bowel disease, *Gut*, 2013, **62**, 209–219.
62. P.R. Dorling, P.S. Quinn and J.D. Judah, Evidence for the coupling of biosynthesis and secretion of serum albumin in the rat. The effect of colchicine on albumin production, *Biochem. J.*, 1975, **152**, 341–348.
63. J. Lee, M.M. Peña, Y. Nose and D.J. Thiele, Biochemical characterization of the human copper transporter Ctr1, *J. Biol. Chem.*, 2002, **277**, 4380–4387.
64. Y. Nose, B.E. Kim and D.J. Thiele, Ctr1 drives intestinal copper absorption and is essential for growth, iron metabolism, and neonatal cardiac function, *Cell Metab.*, 2006, **4**, 235–244.
65. H. Kim, H.Y. Son, S.M. Bailey and J. Lee, Deletion of hepatic Ctr1 reveals its function in copper acquisition and compensatory mechanisms for copper homeostasis, *Am. J. Physiol. Gastrointest. Liver Physiol.*, 2009, **296**, G356–G364.
66. F. Pierrel, P.A. Cobine and D.R. Winge, Metal ion availability in mitochondria, *Biometals*, 2007, **20**, 675–682.
67. K.E. Vest, S.C. Leary, D.R. Winge and P.A. Cobine, Copper import into the mitochondrial matrix in *Saccharomyces cerevisiae* is mediated by Pic2, a mitochondrial carrier family protein, *J. Biol. Chem.*, 2013, **288**, 23884–23892.
68. C.W. Peterson, S.S. Narula and I.M. Armitage, 3D solution structure of copper and silver-substituted yeast metallothioneins, *FEBS Letters*, 1996, **379**, 85–93.

Table 1. Influence of Ag-diet on biochemical and physiological indicators

Parameters	Animal group		
	Control	Ag-A1	Ag-N6
Blood serum			
[Cu], $\mu\text{g/L}$ ($n=10$)	1306 \pm 100	120 \pm 10 (***) ^(a)	981 \pm 28 (***)
[Ag], $\mu\text{g/L}$ ($n=10$)	not assessed	2050 \pm 210	1580 \pm 240
^(b) [Cp] protein, mg/dL ($n=8$)	65 \pm 7	58 \pm 5 (NS)	60 \pm 8 (NS)
^(c) Oxidase activity, mg/dL	38.5 \pm 3.4 ($n=10$)	1.7 \pm 0.5 ($n=15$) (***)	20.0 \pm 0.7 ($n=20$) (***)
^(d) Ferroxidase activity, relative to control ($n=5$)	1.0 \pm 0.23	0.028 \pm 0.013 (*)	0.70 \pm 0.14 (**)
SOD3 activity, U/L ($n=5$)	68 \pm 19	112 \pm 40 (NS)	155 \pm 55 (NS)
Hemoglobin, g/L ($n=5$)	172 \pm 21	168 \pm 15 (NS)	175 \pm 30 (NS)
Reproductive function			
Age of sexual maturity, days	60-70 ($n=40$)	mature from the start of the experiment	60-70 ($n=20$) ^(e)
Number of rats in litter	10 \pm 2 ($n=20$)	drops sharply ^(f)	5 \pm 1 ($n=8$)
Viable fetus	90%	0% ^(f)	90%

^(a) - Significance levels: * – $P < 0.005$; ** – $P < 0.001$; *** – $P < 0.0005$; NS – not significant, $P \geq 0.05$. Ag-A1 was compared to control; Ag-N6 was compared to Ag-A1.

^(b) - determined by rocket immunoelectrophoresis ;

^(c) - determined in *p*-phenylenediamine assay;

^(d) - measured by in-gel assay;

^(e) - males and females were eating Ag-fodder;

^(f) - data cited from Shavlovski et al.⁵⁰

Table 2. The list of amino acids taking part in copper coordination in active centers of human ceruloplasmin, SOD1 and SOD3 (according to X-ray analysis)

Enzyme	PDB ID	Copper ion	Residues that provide R-groups for copper coordination
SOD1	1HL5	Cu	H46, H48, H63 and H120; tetrahedral geometry
SOD3	2JLP	Cu	H96 and H98
Cp*,	1KCW, 2J5W	Cu21 (blue)	H276, C319 , H324
		Cu41 (blue)	H637, C680 , H685
		Cu42 (labile)	D684
		Cu61 (blue)	H975, C1021 , H1026
		Cu62 (labile)	H940, D1025
		Cu31	H163, H980, H1020, [oxygen]
		Cu32	H103, H161, H1022, [oxygen]
		Cu34	H101, H978, H980, [oxygen]

*Ceruloplasmin can contain up to 8 copper atoms, 2 of which are labile. The data on copper binding sites are summarized in the table (amino acid residue and copper atom numbering correspond to the PDB records).

 1
2
3
4
5
6
7
8
9
10
11
12
13
14
15
16
17
18
19
20
21
22
23
24
25
26
27
28
29
30
31
32
33
34
35
36
37
38
39
40
41
42
43
44
45
46
47
48
49
50
51
52
53
54
55
56
57
58
59
60

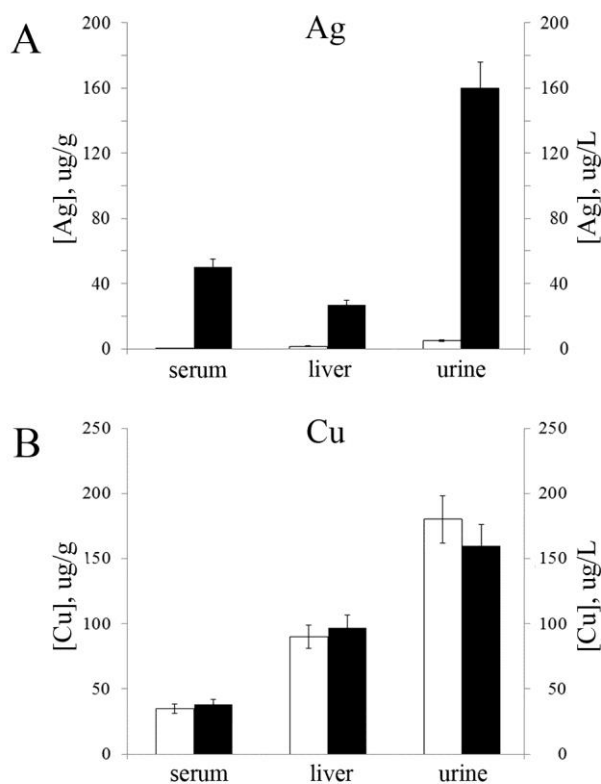


Fig. 1. The distribution of silver (A) and copper (B) in the body of Ag-P10 rats. White bars – control ($n=5$); black bars – Ag-P10 ($n=5$). Ordinate: Ag or Cu concentration, $\mu\text{g/g}$ of the liver tissue, $\mu\text{g/L} \times 0.1$ for serum, and $\mu\text{g/L}$ for urine. The data are displayed as average value \pm S.D.

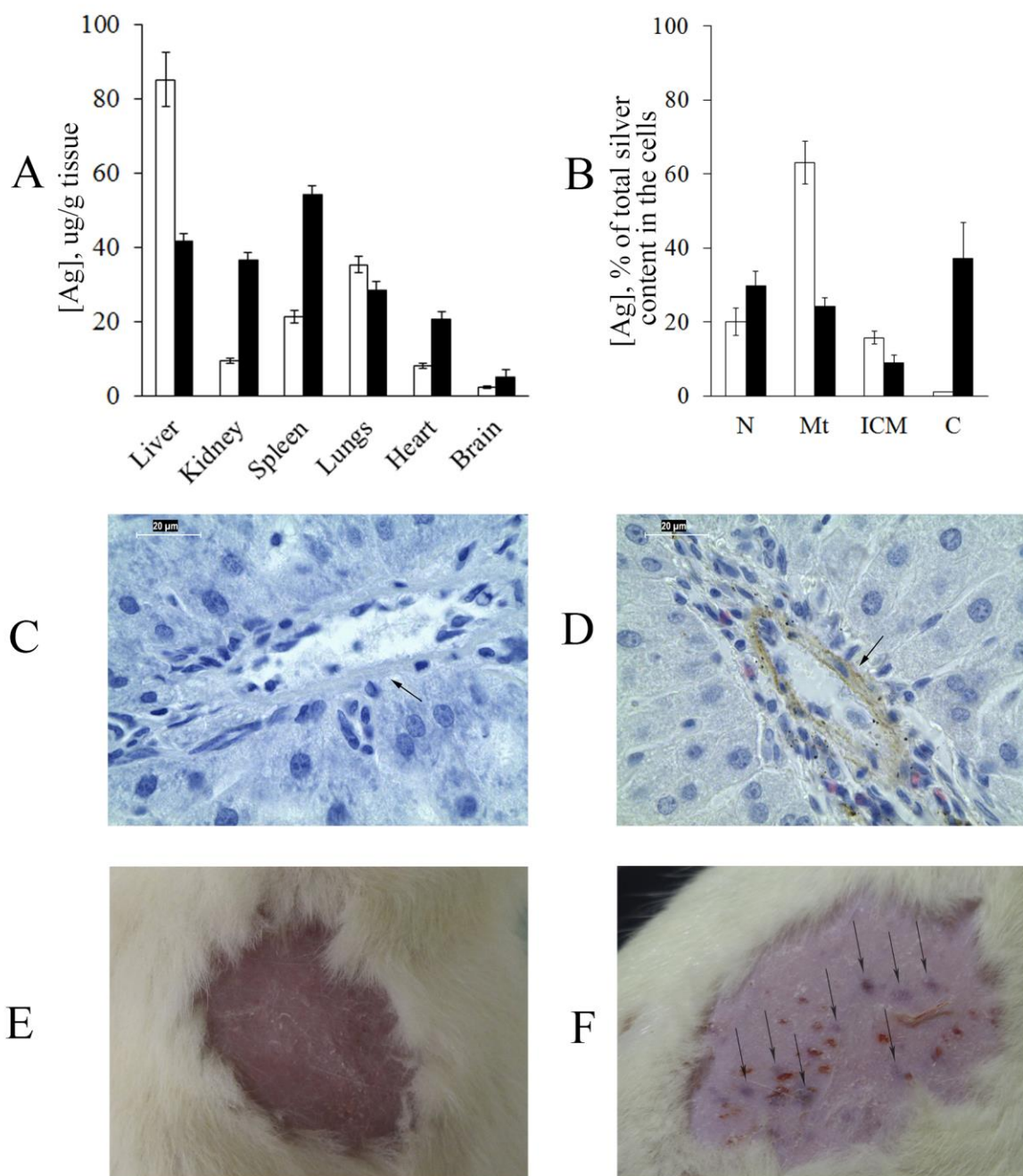


Fig. 2. Silver distribution in the body of Ag-rats.

(A) – Distribution of silver in the body of Ag-rats. Ordinate: silver concentration, $\mu\text{g/g}$ tissue; white bars – Ag-A1 ($n=5$), black bars – Ag-N6 ($n=5$). (B) – Distribution of silver in the liver cells. Ordinate: silver concentration, % of total silver content in the cells; white bars – Ag-A1 ($n=4$), black bars – Ag-N6 ($n=4$). N – nuclei, Mt – mitochondria, ICM – intracellular membranes, C – cytosol. The data are displayed as average value \pm S.D. (C), (D) – Histochemical staining of sections of the liver of Ag-A1 and Ag-N6 respectively. Vascular walls and silver granules are indicated by the arrow. (E), (F) – View of the abdominal skin of Ag-A1 and Ag-N6 respectively. Inclusions in the skin of Ag-N6 rats are shown by the arrows. The other spots are micro trauma after hair pull out.

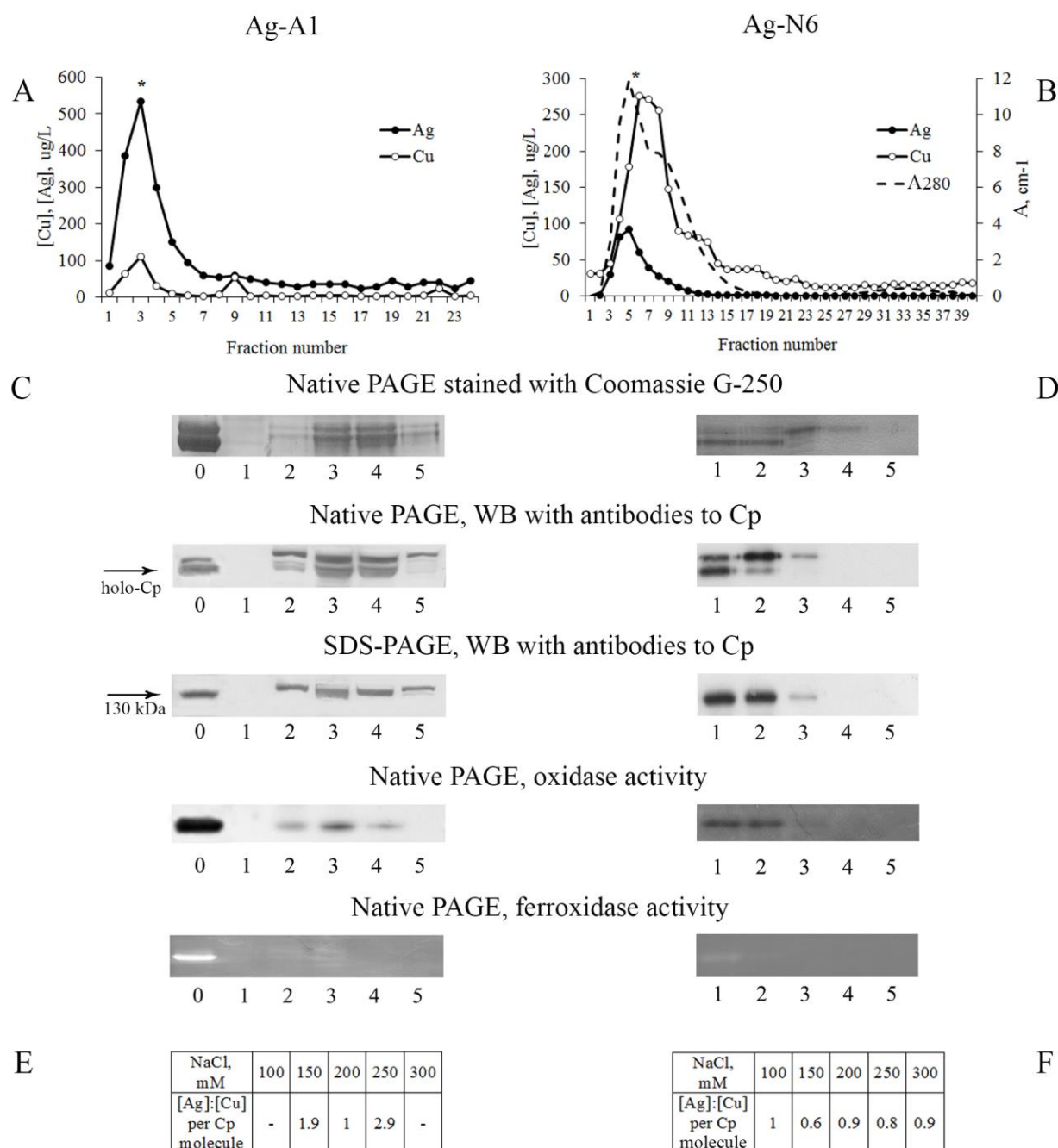


Fig. 3. Distribution of copper and silver in blood serum and Cp fractions.

(A), (B) – Distribution of copper and silver in gel-filtration fractions of the sera of Ag-A1 and Ag-N6 rats respectively. Abscissa: gel-filtration fraction number; ordinate: copper concentration, $\mu\text{g/L}$ (white circles); silver concentration, $\mu\text{g/L}$ (black circles). The asterisk indicates the position of Cp as tested by immunoblotting and oxidase activity assay. Dashed line – A_{280} . (C), (D) – Characteristics of Cp samples, isolated from sera of Ag-A1 and Ag-N6 rats respectively. Lane numbers of DEAE-Sepharose chromatographic fractions: 0 – fraction eluted by 200 mM NaCl from serum of control rats, 1 – 5 – fractions eluted at 100, 150, 200, 250 and 300 mM NaCl respectively. Electrophoresis was carried out in 8% PAG. From top to bottom: native PAGE, 1 μL per lane, gel was stained with Coomassie G-250; the band corresponding to native Cp is

1
2 presented; *native PAGE Western blot (WB)* with antibodies to Cp, 0.1 μL per lane, the arrow
3 indicates position of oxidase Cp; *SDS-PAGE WB* with antibodies to Cp, 0.1 μL per lane; *native*
4 *PAGE* stained with *o*-dianisidine, 1 μL per lane; *native PAGE* stained with Mohr salt/ferrozine,
5 per lane: 10 μL for Ag-A1, 5 μL for Ag-N6. Data in section (C) are reproduced from our
6 previous work.²⁸ (E) – Atomic copper/silver ratios in the eluted Cp fractions of Ag-A1. (F) – the
7 same indicators for Ag-N6 rats. Cp concentration was determined by rocket
8 immunoelectrophoresis. Concentration of metals was determined by FAAS.
9
10
11
12
13
14
15
16
17
18
19
20
21
22
23
24
25
26
27
28
29
30
31
32
33
34
35
36
37
38
39
40
41
42
43
44
45
46
47
48
49
50
51
52
53
54
55
56
57
58
59
60

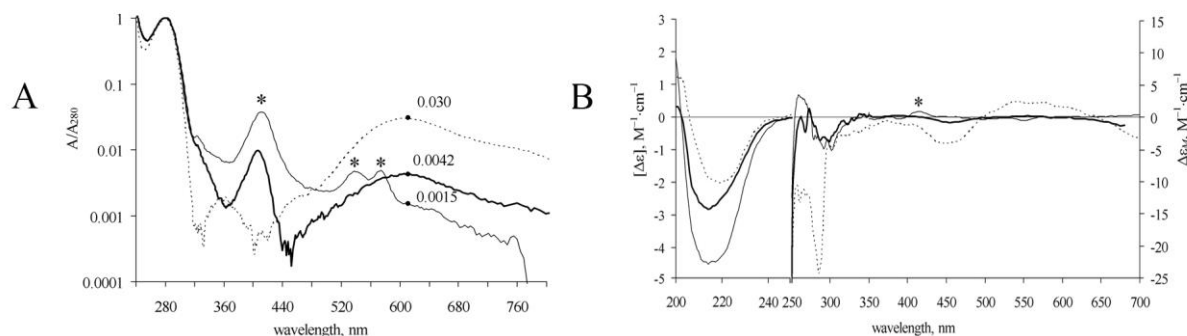


Fig. 4. UV-Vis absorption (A) and circular dichroism (B) spectra of Cp samples with largest Cp concentration: 200 mM NaCl fraction from sera of Ag-A1 rats (thin line) and 100 mM NaCl fraction from sera of Ag-N6 rats (thick line). A spectrum of Cp preparation from control rats is shown by dotted line. Absorption spectra are shown with Rayleigh scattering removed. Asterisks indicate peaks of trace hemoglobin impurities.

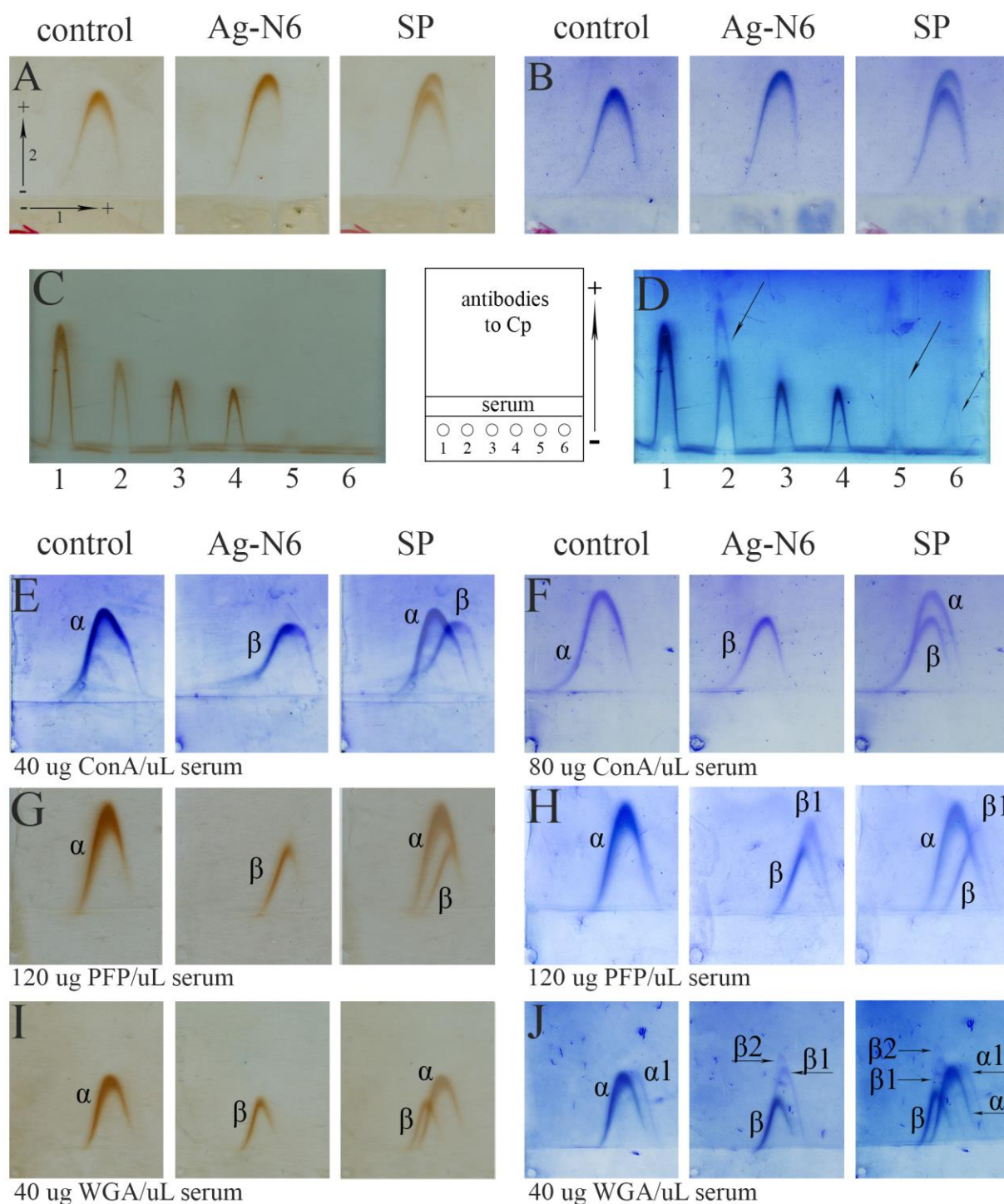


Fig. 5. Some properties of Ag-N6 Cp.

(A) – 2D-immunoelectrophoresis of serum from control and Ag-N6 rats; SP – 50%:50% superimposed image. 1.5 μ L serum aliquots were loaded into wells. Gels were stained with o-dianisidine. Arrows indicate the order of directions and polarity. (B) – The same gels were stained with Coomassie G-250. (C) – Cross-immunoelectrophoresis (the details are described in Methods). The wells were loaded with: (1) 1.5 μ L of control serum and (2) 1.5 μ L of Ag-N6 serum; (3) 0.05 μ L of 200 mM NaCl fraction of holo-Cp ($A_{610}/A_{280}=0.045$); (4) 1 μ L of 100 mM

1
2 NaCl fraction of Ag-N6 Cp; (5) 5 μ L of 150 mM NaCl fraction of Ag-N6 Cp, (6) 5 μ L of 200
3 mM NaCl fraction of Ag-N6 Cp. Gel was stained with *o*-dianisidine. (D) – the same gel stained
4 with Coomassie G-250. Arrows indicate the oxidase-negative zones. In the middle – the schema
5 of cross-immunoelectrophoretic gel. (E – J) – 2D-affinoimmuno-electrophoresis. The wells were
6 loaded with 1.5 μ L of serum. (E) – Serum aliquots were pre-incubated with 40 μ g ConA per 1
7 μ L serum, (F) – the same, but with 80 μ g ConA per 1 μ L serum. (G), (H) – Serum aliquots were
8 pre-incubated with 120 μ g PFP per 1 μ L serum. (I), (J) – Serum aliquots were pre-incubated with
9 40 μ g WGA per 1 μ L serum. (G), (I) – gels were stained with *o*-dianisidine. (E, F, H, and J) –
10 gels were stained with Coomassie G-250. Greek letters designate the immunoprecipitation zones.
11 Each sample was combined from equal volumes of sera of three rats (control and Ag-N6
12 respectively). Each pair of samples (control, Ag-N6) was analyzed at least twice; the replicas had
13 similar positions of the zones.
14
15
16
17
18
19
20
21
22
23
24
25
26
27
28
29
30
31
32
33
34
35
36
37
38
39
40
41
42
43
44
45
46
47
48
49
50
51
52
53
54
55
56
57
58
59
60

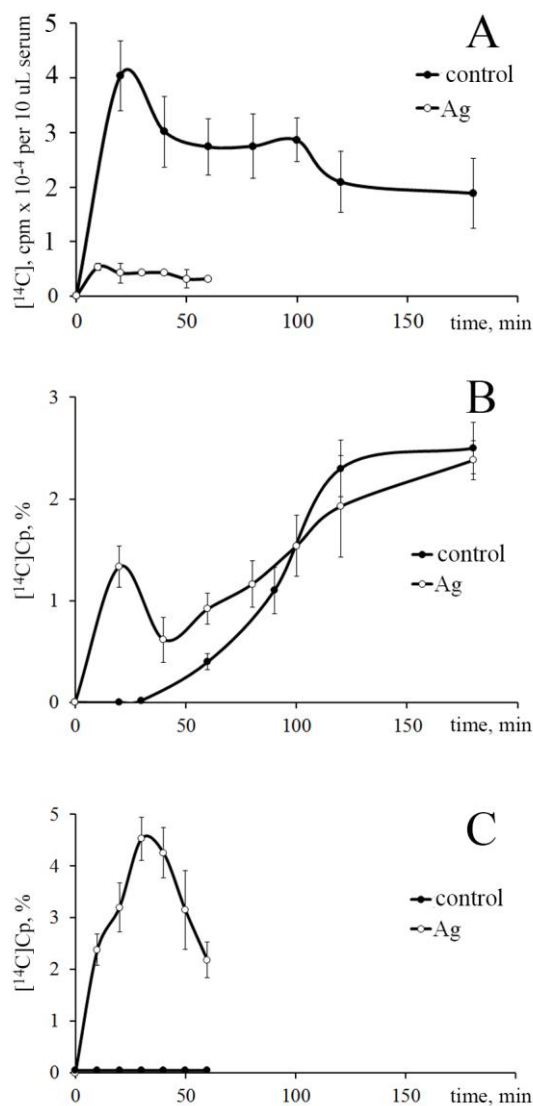


Fig. 6. Secretion rate of *de novo* synthesized Cp forms in Ag-N6.

(A) – Dynamics of the appearance of *de novo* synthesized proteinaceous $[^{14}\text{C}]$ products in bloodstream: black circles – serum samples were collected from tail vessels of Ag-N6; white circles – serum samples were collected from catheterized carotid artery of Ag-N6 rat with liver isolated from circulation. Abscissa: time, min, after administration of the $[^{14}\text{C}]$ -amino acid pulse dose; ordinate: $[^{14}\text{C}]$ radioactivity, $\text{cpm} \times 10^{-4}$ per 10 μL serum. (B) – Dynamic appearance of *de novo* synthesized Cp in circulation: black circles – control, white circles – Ag-N6. Abscissa: time, min; ordinate: $[^{14}\text{C}]$ Cp, %. (C) – Dynamics of the appearance of *de novo* synthesized Cp in circulation of the rats with liver isolated from bloodstream: black circles – control rats, white circles – Ag-N6 rats. Abscissa: time, min; ordinate: percentage of $[^{14}\text{C}]$ Cp in $[^{14}\text{C}]$ total protein. Two replica of the experiment are presented, error bars indicate average deviation.

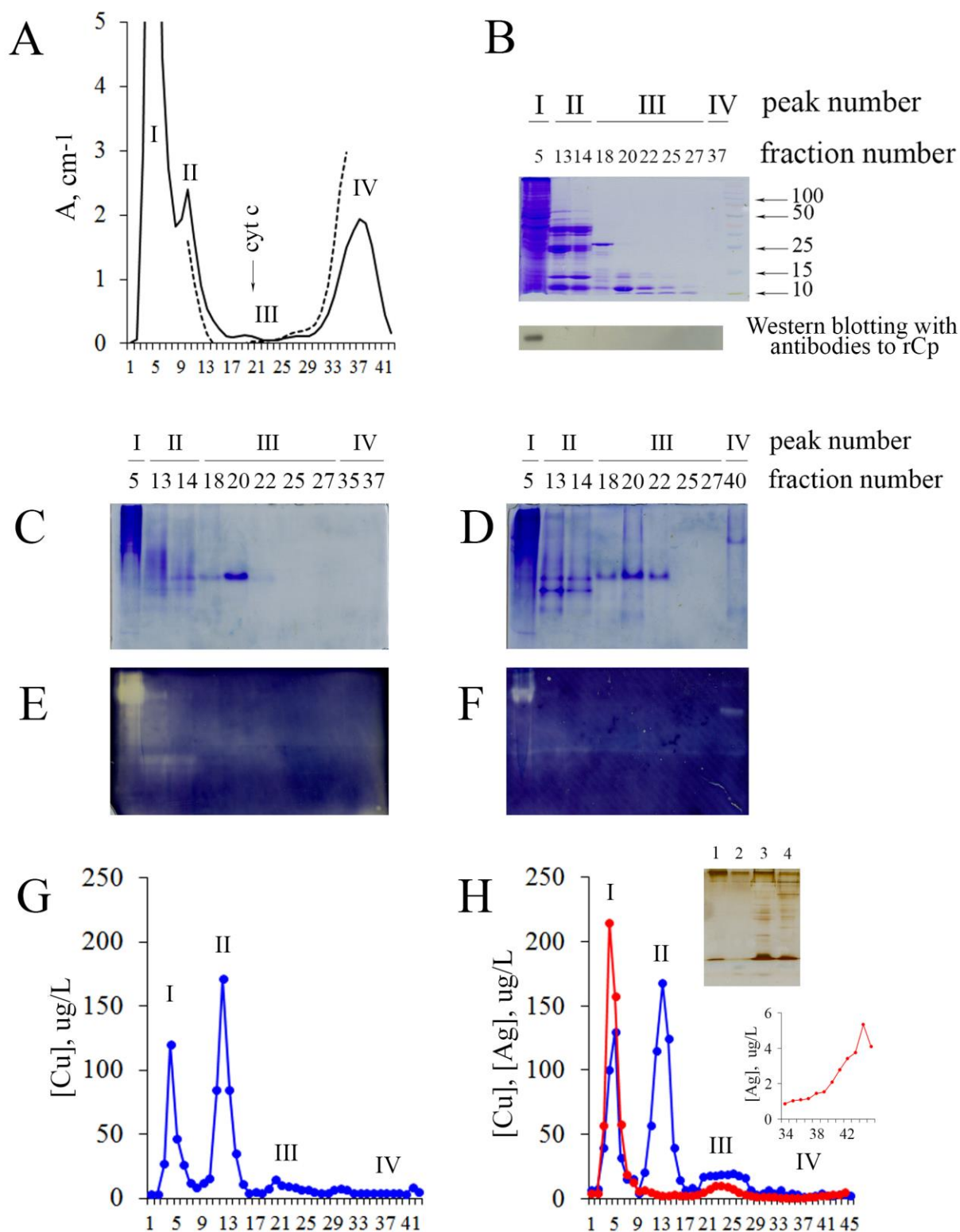


Fig. 7. The distribution of silver and copper in liver cell cytosolic fraction.

(A) – Absorption profiles of gel-filtration chromatogram of cytosol from the liver cells of control rats. Abscissa: fraction number; ordinate: A_{280} (solid line) and A_{254} (dotted line). The arrow indicates elution peak of cytochrome *c*. (B) – SDS-PAGE of selected fraction from the peaks; *Top* – Coomassie staining, *bottom* – Western blotting (WB) with antibodies to rat Cp (rCp). (C) – Non-denaturing PAGE of the same fractions. (D) – Non-denaturing PAGE for the analogous

1
2 fractions for Ag-N6 rats. (E), (F) – SOD activity in the gels displayed in sections (C) and (D)
3 respectively. (G) – Copper concentration profile in the chromatogram of control rats. (H) –
4 Copper (blue line) and silver (red line) – concentration profile in the chromatogram of Ag-N6
5 rats; abscissa: fraction number; ordinate: metal concentration, $\mu\text{g/L}$. Insets to section (H), *Top*:
6 12% SDS-PAGE of fractions from peak IV of control (1 and 2) and Ag-N6 (3 and 4) stained
7 with AgNO_3 . The samples were treated by SDS and 2-ME at 95 °C, 5 min (1 and 3) or incubated
8 at room temperature during 5 min (2 and 4); *Bottom*: magnified plot of silver concentration in
9 Peak IV.
10
11
12
13
14
15
16
17
18
19
20
21
22
23
24
25
26
27
28
29
30
31
32
33
34
35
36
37
38
39
40
41
42
43
44
45
46
47
48
49
50
51
52
53
54
55
56
57
58
59
60

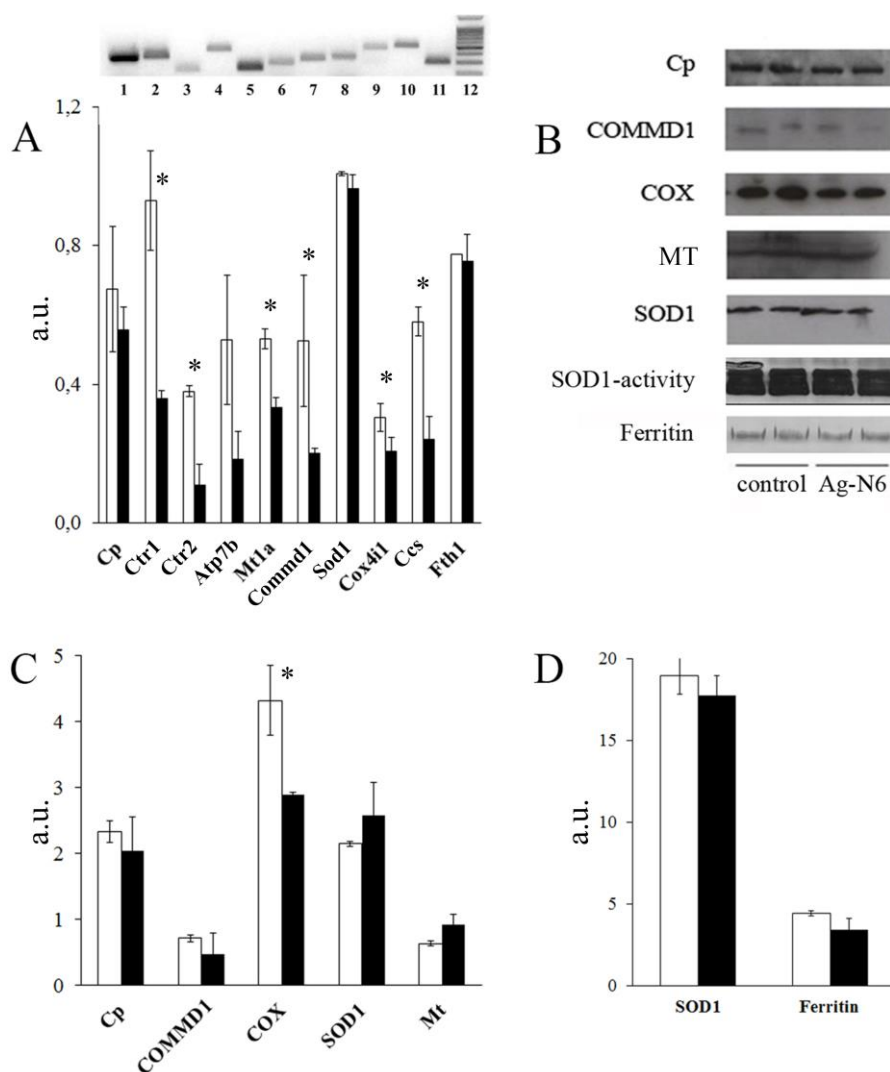


Fig. 8. Expression of genes associated with copper metabolism in the liver of control (white bars) and Ag-N6 (black bars) rats.

(A) – Bar plot for relative content of mature transcription products, abscissa indicates gene names. The sample image of the gel with PCR products is displayed above the diagram, Lane 1 – β -actin, lanes 2-11 – genes in the same order as in the bar blot, lane 12 – markers, bold band corresponds to 500 bp. Each value was combined from 3 independent PCR replicas of cDNA samples, isolated from 3 animals. (B) – Immunoblotting of Cp (blood serum 0.1 μ L/well), COMMD1 (40 μ g cytosol protein/well), COX (20 μ g mitochondrial protein/well), MT (50 μ g cytosol protein/well), SOD1 (30 μ g cytosol protein/well), enzymatic activity of SOD1 (100 μ g cytosol protein/well), and the level of ferritin iron loading (150 μ g cytosol protein/well). Gels assayed for SOD1 are presented as negative images. Ferritin was stained with $K_4Fe(CN)_6$; (C), (D) – Semi-quantitative analysis of data, presented in section (B). The data in (A), (C) and (D) are displayed as average value \pm S.D ($n = 3$) in arbitrary units (a.u.). Asterisks indicate significant changes, $P < 0.05$.